REPUBLIC OF IRAQ

MINISTRY OF HIGHER EDUCATION

AND SCIENTIFIC RESEARCH

AL-FURAT AL-AWSAT TECHNICAL UNIVERSITY

Design and Analysis of MIMO Optical Visible Light Communication with Based On Neural Network

A THESIS

SUBMITTED TO THE COMMUNICATION TECHNIQUES ENGINEERING DEPARTMENT

IN PARTIAL FULFILLMENT OF THE REQUIREMENTS FOR THE TECHNICAL MASTER DEGREE

IN

COMMUNICATION TECHNICAL ENGINEERING

BY

Mustafa Aqeel Abbas

(B. Sc. Communication Eng.)

Supervised by

Prof. Dr. Ali A. Al-Bakry

Asst. Prof. Dr. Bashar J. Hamza

December 2019

جمهورية العراق

وزارة التعليم العالي والبحث العلمي

جامعة الفرات الاوسط التقنية

الكلية التقنية الهندسية– نجف

تصميم وتحليل المدخلات المتعددة والمخرجات المتعددة للاتصال بالضوء المرئي البصري باستخدام الشبكة العصبية.

رسالة مقدمة الى

قسم هندسة تقنيات الاتصالات

كجزء من متطلبات نيل درجة ماجستير تقني في هندسة الاتصالات

تقدم بها

مصطفى عقيل عباس

بكالوريوس في هندسة الاتصالات

إشراف

أ .د	أ. م .د
علي عبد العباس البكري	بشار جابر حمزة

كانون الاول/ 2019

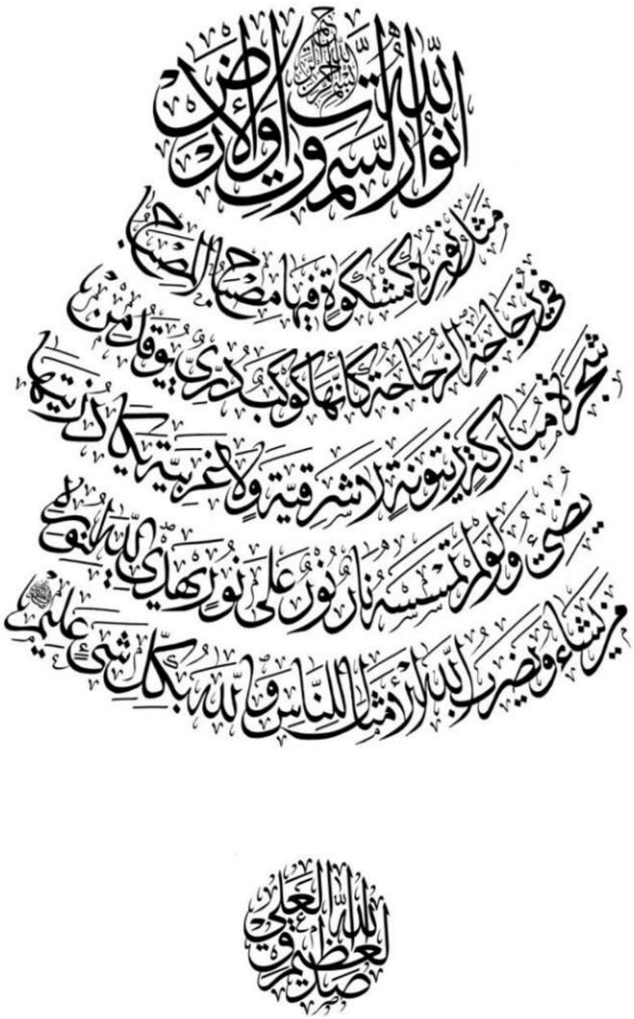
الله نور السموات والأرض
مثل نوره كمشكوة فيها مصباح المصباح
في زجاجة الزجاجة كأنها كوكب دري يوقد من
شجرة مباركة زيتونة لا شرقية ولا غربية يكاد زيتها
يضيء ولو لم تمسسه نار نور على نور يهدي الله لنوره
من يشاء ويضرب الله الأمثال للناس والله بكل شيء عليم
صدق الله العظيم

Dedication

To the greatest person that Allah has ever created,

Prophet Mohammad (P) .

To the best person that Allah has ever created after His Prophet,

Imam Ali (P).

To my AL-Furat Al-Awsat Technical University ,and my Engineering Technical College.

To my beloved Parents, my wife ,my sons, my brothers, and my friends

To all who supported and encouraged me to achieve my success.

Acknowledgment

First, I want to express my sincere gratitude to my advisor, **Prof. Ali A. Al-Bakry** and **Asst. Prof. Bashar J. Hamza** and **Asst. Prof. Faris Mohammed Ali** for the continuous support of my M.Sc. study, and relating research, for his patience, motivation, and vast acknowledgment. Their guidance helped me in all the period of the research and writing of this thesis. I could not have imagined having a better advisor and mentor for my M.Sc. Study. Thank you for your faith in me in the toughest situations.

My sincere thanks also go to **Dr. Salim. M. Wali** Head of Technical Electrical Engineering Department, who provided me an opportunity to be under his supervision, and who was gave access to the laboratory and research easiness. Without his invaluable support, it cannot be possible to conduct this research.

Last but not least, I would like to thank my family: my parents and to my brothers and sister and my wife for supporting me spiritually throughout writing this thesis and my life in general.

Supervisor Certification

I/We certify that this thesis titled **" Design and Analysis of MIMO Optical Visible Light Communication with Based on Neural Network "** which is being submitted by **Mustafa Aqeel** was prepared under my/our supervision at the Communication Techniques Engineering Department, Engineering Technical College-Najaf, AL-Furat Al-Awsat Technical University, as a partial fulfillment of the requirements for the degree of Master of Technical in Communication Engineering.

Signature:

Name: **Ali A. A. Al-Bakry**

(Supervisor)

Date: / / 2019

Signature:

Name: **Bashar J. Hamza**

(Supervisor)

Date: / / 2019

In view of the available recommendation, I/we forward this thesis for debate by the examining committee.

Signature:

Dr. Salim M.Wali

(Head of Communications Tech. Eng. Dept.)

Date: / / 2019

Committee Report

We certify that we have read this thesis titled **" Design and Analysis of MIMO for Optical Visible Light Communication with Based on Neural Network "** which is submitted by **Mustafa Aqeel Abbas** and as Examining Committee, examined the student in its contents. In our opinion, the thesis is adequate for award of degree of Master of Technical in Communication Engineering.

Signature:
Name: **Asst. Prof. Dr**. **Ali A. Al-Bakry**
Supervisor
Date: / / 2019

Signature:
Name: **Asst. Prof. Dr. Bashar J. Hamza**
Supervisor
Date: / / 2019

Signature:
Name: **Asst. Prof. Dr. Ahmed Kareem Al-Bakry**
(Member)
Date: / / 2019

Signature:
Name: **Dr. Hussam Noman Mohammed Ali**
(Member)
Date: / / 2019

Signature:
Name: **Asst. Prof. Dr. Musa H. Wali**
(Chairman)
Date: / / 2019

Approval of the Engineering Technical College Najaf

Abstract

A Visible Light Communication is a concept used to describe the systems of wireless communication that transmitting information in modulating the light that is visible for human eyes. One of the key problems of indoor VLC systems is achieving uniform communication performance at different locations without affecting the primary illumination function. In addition, the radio spectrum is very busy and have limitation in data rate in communication networks system, so, it becomes increasingly difficult to find the wireless capability to support wireless data transfers for media applications and, Multi-User Interference (MUI) in the communications system. In this work, developed a method that was divided into two parts. The first part is a new algorithm called Neural network Coordinate Evaluator Algorithm (NNCEA) for achieving high accuracy positioning and the second part is a new algorithm in channel coding called New Line Neural Network System (NLNNS) for achieving Multi input-Multi output system (MIMO) by using OFDM. Where in NNCEA used the neural network to specify the location of the user in the room used for testing and giving better SNR and BER .while the NLNNS used the QAM modulation with modulation index (M=4,8,16)with Discrete Fourier Transform –Spread (DFT-S-OFDM) to achieve MIMO-OFDM. According to the Results in this work , improved the accuracy of the site calculation from 10 to 15 cm as well as improved positioning accuracy outside the cell. So this is lead to enhance data rate, While, by using the second part of MIMO–OFDM system that leads to enhancing the SNR reach to (0.95 dB) and BER more than 10^{-5}, which are introduced to eliminate multi-user interference (MUI).

الخلاصة

إن اتصال الضوء المرئي (VLC) هو مفهوم يستخدم لوصف أنظمة الاتصالات اللاسلكية التي تنقل المعلومات في تعديل الضوء المرئي للعين البشرية. تتمثل إحدى المشكلات الرئيسية لأنظمة VLCالداخلية في تحقيق أداء اتصال موحد في مواقع مختلفة دون التأثير على وظيفة الإضاءة الأساسية. بالإضافة إلى ذلك ، فإن الطيف الراديوي مشغول للغاية وله معدل بيانات محدود في نظام شبكات الاتصالات ، لذلك ، يصبح من الصعب بشكل متزايد العثور على القدرة اللاسلكية لدعم نقل البيانات اللاسلكية لتطبيقات الوسائط وتداخل متعدد المستخدمين (MUI) في الاتصالات النظام.

في هذا العمل ، تم بتطوير طريقة تنقسم إلى جزأين ، الجزء الأول خوارزمية جديدة تسمى الشبكة العصبية خوارزمية مقيم الإحداثيات (NNCEA) لتحقيق دقة عالية في تحديد المواقع والجزء الثاني خوارزمية جديدة في ترميز القناة تسمى هذه الخوارزمية نظام الشبكة العصبية الجديدة (NLNNS) لتحقيق متعدد المدخلات متعدد نظام الإخراج (MIMO) باستخدام OFDM .حيث يستخدم NNCEA الشبكة العصبية لتحديد موقع المستخدم في الغرفة التي تستخدم للاختبار وإعطاء أفضل SNR و BER. في حين يستخدم NLNNS تضمينQAM مع مؤشر تضمين (M = 16،8،4) مع تحويل فوريه المنفصل - انتشار OFDM (DFT-S-OFDM) لتحقيق MIMO-OFDM.وفقًا للنتائج في هذا العمل ، تم بتحسين دقة حساب الموقع من 10 إلى 15 سم بالإضافة إلى تحسين دقة تحديد المواقع خارج الخلية. لذلك هذا يؤدي إلى تعزيز معدل البيانات . بينما ، باستخدام الجزء الثاني من نظام MIMO – OFDM الذي يؤدي إلى تعزيز SNR تصل الى (0.95 دسي بيل) و BER اكثر من 10^{-5}، والتي تقدم للقضاء على التداخل متعدد المستخدمين (MUI).

Contents

List of Figures

List of Tables

Nomenclature

Symbol	Definition	Unit
ARX	The active photodiode area	mm
Bn	The noise bandwidth	Hz
Ba	The Amplifier bandwidth	Hz
C	The number of channels	----
f	The cost function of the activation	----
h_{dist}	The distance between transmitter and receptor	m
h	Impulse response	----
I_{amp}	The Amplifier noise density	$A/Hz^{0.5}$
I	The luminous intensity in angle	degree
I_0	The center luminous intensity of an LED	----
Lamp	The luminous	Cd
M	Modulation index	----
Pr_{Total}	Total received power	W
Pr_{Los}	The Received power of LOS	W
Pr_{diff}	The Received power of diffusion	W
P_{LED}	The power emitted by the LED	W

P_{amp}	The ambient light power.	W
q	The Electron charge	C
Rr	The Photodiode responsivity	A/W
Ro	The Lambertian radiant intensity	W/Sr^{-1}
Greek Symbols		
φ	The Transmitter Semi-angle (FOV)	degree
θ	The incident angle	degree
σ_T	Total noise variance	dB
σ_{shot}	The Shot-noise variance	dB
$\sigma_{amplifier}$	The Amplifier noise density	dB
tanh	Hyperbolic tangent	----

Abbreviations

Symbol	Description
BER	Bit Error Rate
CSI	Channel State Information
CP	Cyclic prefix length
DFFT-S-OFDM	Discrete Fourier Transform Spread OFDM
FL	Full-Layer
FOV	Field Of View
MIMO	Multiple Input Multiple Output
ML	Machine Learning
NNCEA	Neural Network Coordinates Evaluator Algorithm
NLNNS	New Line Neural Network System
NNS	Neural Network System
OFDM	Orthogonal Frequency Division Multiplexing
OWC	Optical Wireless Communication
RSS	Receive Signal Strength
RLU	Rectified Linear Unit
SNR	Signal-to-Noise Ratio
PD	Photodetector
TDE	Time-Domain Equalization

List of Publications

1) **High Precision Indoor Positioning System of VLC Using Neural Network /(Al-Qadisiyah Journal for Engineering Sciences) in Al-Qadisiyah university**

   (Submitted)

2) Theoretical Approach for MIMO -VLC System using OFDM and Neural Network / (IOP Conference Series: Materials Science and Engineering.

(Accepted)

CHAPTER ONE

INTRODUCTION

1.1 Background of VLC

A visible light communication (VLC) is a concept used to describe the systems of wireless communication that transmitting information in modulating the light that is visible for eyes human [1]. Light primarily serves as a source of illumination rather than communication, which may not be the chief purpose. The growth of visible light-emitting diodes (LEDs) for illumination growth to interesting in studying VLC that grew rapidly. When the room be already illuminated by LEDs. So sharing of resources not only reduces the required hardware cost also saves electric power. In the last years, VLC technology developed both in industry and academics [2]. The main aim of this technology is the increasing popularity of LEDs because of their long lifetime, energy efficiency, high data security, and environmental friendliness. In reality, using visible light as one of the wireless communication media is not new [3]. The first electronic wireless communication that used sunlight as its light source was successfully developed by since Alexander Graham Bell, who was invented a photophone in 1880 [4]. By this new invention using sunlight beams enabled transmissions of modulated voice data over the distance of 200 m, In this invention itis an obvious drawback because it relied on sunlight that is available intermittently in a day. Since then, much additional enhancement has been made based on the Bell design like the use of a tungsten lamp with an infrared (IR) filter, mercury, and high-pressure vapor [5]. After that, fluorescent lights with low data rates were also used for communication [6]. In the 1990s, high-brightness LED lamps were introduced for its general lighting functions. In the following years, LED luminous efficiency improved rapidly, and the life-time was up to 100,000 hours [7]. After the rapid development of solid-state lighting, he introduced the concept

of visible light communication in 2003 at the Nakagawa Lab at Kew University, which has been overshadowed by its growing development in both academic and industrial circles on a global scale .In 1999, Pang et al. the concept of VLC conceived includes modulation signals on fast-switching LEDs. As described in VLC systems with LED lights implemented, the wireless transmission service can be provided in the open space for voice messages. In 2001, a free technology project called Reasonable Optical Near Joint Access (RONJA) was developed at Kulhavy of Twibright Labs to create reliable optical data links at a distance of 1.4 km in free space using visible light. As a result, the connection speed can reach 10 Mbps [8]. By switching between white phosphorescent LED and high-speed lighting, a data rate of up to 40 Mbps can be achieved easily. Using the same on-off keying system (OOK), the white RGB LEDs deliver a data rate higher than 100 Mbps. At the beginning of 2000, data transmission was reported at 400 Mbps by Tanaka et al. Based on the numerical analysis and computer simulations, utilizing white LEDs for both lighting and data communications Over the past few years [9], high data rates in terms of gigabits per second have become possible for VLC systems that have implemented the correct modulation, line coding schemes used, and equations used in transmitters and receivers [10].

VLC technology is derived from and consolidated with the help of several initiatives. Omega is a project in Europe run by researchers coming from universities, research institutions, and technology companies. It aims to develop a home access network or office access network that can provide extensive bandwidth services and transmission speed reach 1Gbps by using a blending of power cables, wireless signals, and light. The Li-Fi consortium

that began in 2011 is sparing no effort in introducing wireless optical technology and guiding this new technology to market.

1.2 Characteristic of VLC

The characteristics of the channel are based on room size and material characteristics of the reflective surfaces, and the same mobile VLC station may experience different performance at different locations**.** One of the main problems of internal VLC systems is to achieve unified connection performance to varying positions without affecting the essential lighting function. Light performance is compared with different ceiling plans for LED array arrangement [11]. A new LED lamp with 12 LED lights evenly distributed over a circle and four LED bulbs in the corner is proposed to reduce SNR uniformity, ensuring that users achieve nearly identical communication quality [12]. Two interior lighting systems are compared using square and hollow designs, indicating that there is an excellent possibility of improving the star design within the room [13]. [14] Modern lighting design is based on four LED lights placed in the corner of the room, and one LED lamp is placed in the middle of the area to distribute the light uniformly. In [15], the lighting properties are analyzed using rectangular and circular LED arrangements with the alterable distance between the lamps and center of the ceiling. An algorithm-based evolutionary improvement scheme is proposed to achieve uniform power received distribution and illumination on the communication floor, as shown in [16].

1.3 Compare between the RF and VLC Communication

RF communication is the most common technology today, but it yet has some notable drawbacks as shown in Table 1.1 .

Table 1.1 Compare between the RF and VLC Communication

NO.	Characteristics	VLC	RF
1	Capacity	visible light range can provide a bandwidth of 400 THz (375-780 nm), which is much larger than the RF band	Radio waves have only a limited range bandwidth is available and expensive (3 KHz – 300GHz).
2	Cost	The devices of transmitter and receiver, which used in the VLC system are cheap compared with RF units.	The devices of transmitter and receiver in the RF unit are expensive compared with VLC system.
3	Efficiency	VLC expends less energy efficient because lighting and data transfer can be done at the same time.	Radio waves that are expend highly energy efficient
4	Safety	VLC is safety and have no affected on equipment in hospitals and instruments in airplanes, and it cannot be hazardous during	Radio waves generate EMI that is seriously affected on equipment in hospitals and instruments in airplanes, and it can be hazardous during

		operations, like oil or gas drilling, nuclear generation, and coal mining.	operations, like oil or gas drilling, nuclear generation, and coal mining.
5	**Human Health**	VLC will be not dangerous health risks to humans and an engaging candidate in consumer service systems.	The RF transmission power cannot be very high because, after increasing the RF power at a given level, there will be dangerous health risks to humans.

1.4 Compare between VLC and Infrared (IR) communication

Infrared(IR) communication is another popular candidate to discuss data transmission. There are various points between VLC and Infrared (IR) communication as shown in Table 1.2 :

Table 1.2 : Compare between VLC and Infrared (IR) communication

NO	Characteristics	VLC	IR
1	**Distance**	The range of VLC systems more than 10m of communication distance	the range of infrared systems can reach only 3m for effective distance.

2	**Noise source**	there are different sources of noise because of the wavelength of the light source in VLC, sunlight, and other sources of light can be noise sources.	The infrared communication noise mainly comes from ambient light that contains infrared light
3	**Data rate**	The VLC communication operates with a rate reach up to 100 Mb/s	Infrared (IR) work while a rate 20Mb/s
4	**Services**	The VLC technology can be used for illumination, data communication, and, positioning	The infrared(IR) has only a communication function.

1.5 Current and Possible Visible Light Applications

The VLC indoor and outdoor applications used can benefit including indoor location, vehicle communication, power line communication, etc.

Office and Home: the data rate desired by each device is increasing rapidly because many people carry on one or more than wireless device at any time like smartwatches, tablets smartphone, smart glasses, etc. Humans spend most of the time in their buildings where the practical application of self-visible light communication technology is where visible light communication is a strong alternative to wireless communication because another function can be added with lighting to LED structure in offices and residential buildings with ease. In Fig 1.1, an example of a local area network(LAN) is published where a laptop, smartphone, and smart glass that can be using VLC are connected.

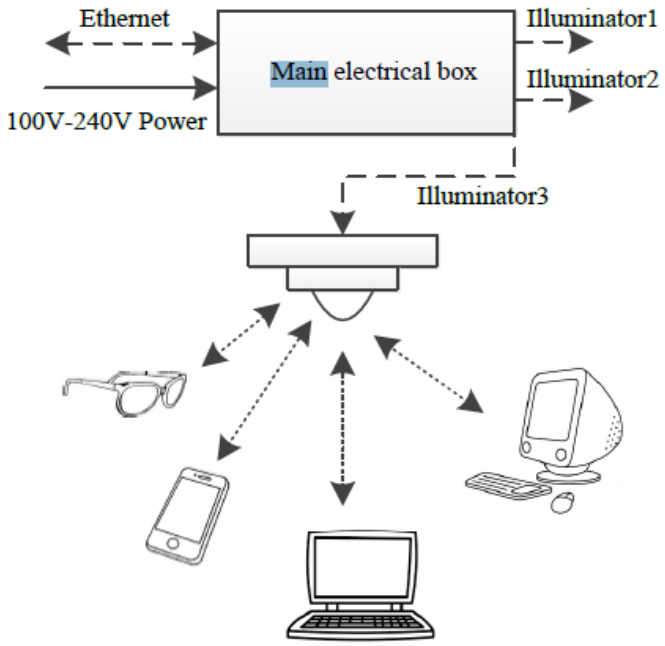

Figure 1.1: VLC used in Office and Home Network [17]

Transport Systems: The used headlights and rear lights for vehicles such as transmitters, cameras, and cameras as a receiver, inter-vehicle communication can be enabled to share information between drivers around tracks, speed, locomotive and destinations to prevent accidents and traffic jams as shown in figure 1.2.

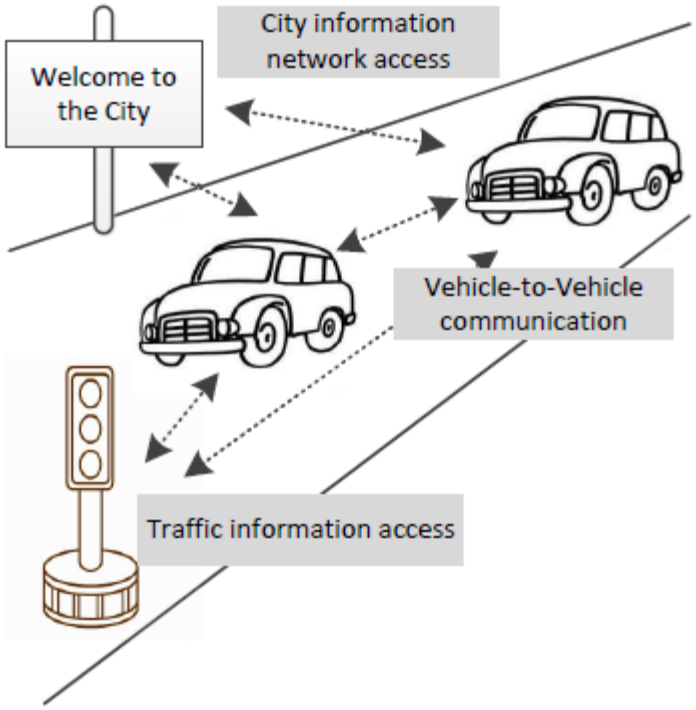

Figure 1.2 VLC used in transportation systems [18]**.**

Another favorable application can be created using aircraft-based in lighting to broadcast music, video, and data exchange with wired terminals in the cabin, which can provide passengers with a better experience. .

Public places: Museums, shopping malls, theatres, and public areas can be equipped with precision navigation systems using visible light, also called visible light position. These navigation systems help shoppers reach new or low goods in the supermarket, guiding the audience to their seats in the theatre . Also, it is used in an emergency to transmit useful information.

1.6 Motivation:

To achieve the best communication between user and internet service provider through light, it must specify the best way which, the light selected to reach users.one of the problems that will reduce the quality of contact is the obstacles between sender and receiver. These obstacles also affect the speed of contact so, for the mentioned reasons, there is a persistent need to determine the position of receiver to avoid losing contact and to achieve higher SNR and BER.

Another way has been taken in consideration to solve the problem by using MIMO to enhance the channel performance ,to highlight how this field of science is fresh and has the interest of researcher, a statistic for the published researches in each year for the VLC has been made by PubMed .show every published paper in each single year.

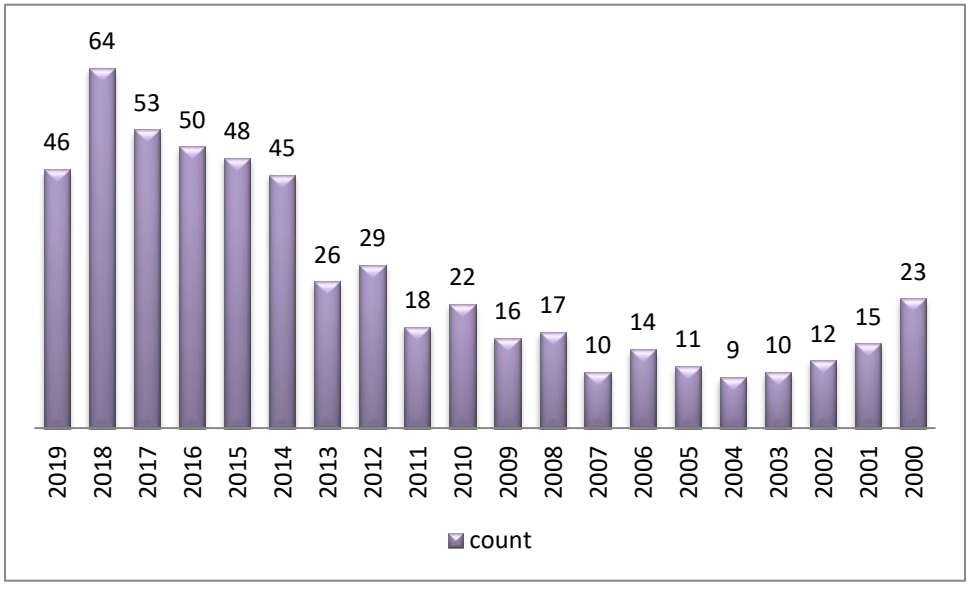

Figure 1.3 published paper in each single year

1.7 Statement of the Problem

1) One of the key problems of indoor VLC systems is achieving uniform communication performance at different locations without affecting the primary illumination function.
2) Radio spectrum is very occupied, and data rate limitation in communication networks, so it becomes increasingly difficult to find the wireless capability to support wireless data transfers for media applications.
3) Multi-User Interference (MUI) in a communications system.

1.8 Scope of Work

The scope of the proposed work is shown in fig (1.3)

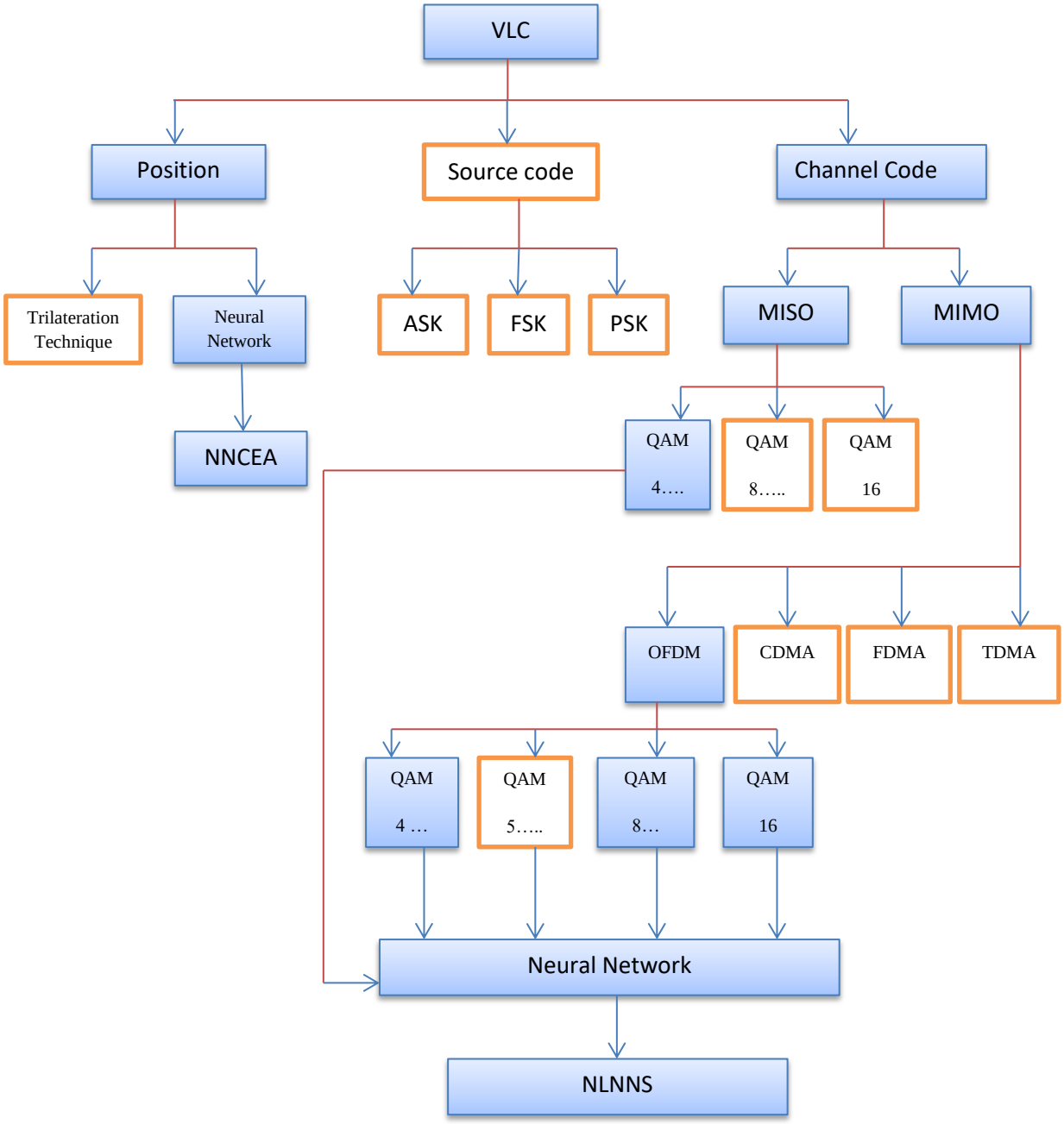

Figure 1.4 The scope of study

1.9 Thesis Objectives:

1) To achieve a high data rate for visible light communications of multi-input and multiple outputs.

2) To eliminate multi-user interference (MUI).

3) To enhancement Power received, SNR and BER in Li-Fi**.**

1.10 Contribution

In this work, in both algorithms we made a contribution.

1) improve the accuracy of the positioning and increase the bandwidth.
2) Signal to noise ratio (SNR) was increased and the Bit error rate (BER) was reduced to more than 10^{-5} .
3) Eliminating the multi users interference (MUI) .

1.11 Thesis Outline:

Chapter 1 general introduction and characteristics of VLC system .as well as, problem statement objective thesis.

Chapter 2 discusses the history of the VLC system in term the methods the researcher used and the result that obtained in previous years.

Chapter 3 discusses our methodology which is divided into two main parts. The first part for positioning and the second for channel coding.

Chapter 4 discusses the results which, obtained from our method that has been mentioned in chapter 3.

Chapter 5 discusses the conclusions and future work for our method.

CHAPTER TWO

THEORETICAL BACKGROUND AND LITERATURE REVIEW

2.1 Introduction of VLC Systems

The spectrum is the rare currency of telecom engineers. At present, with the rapid growth of wireless communication, the problem of using spectrum has become more efficient. Numerous solutions were proposed to solve this problem. One of these solutions is to use visible light frequencies to send data. These frequencies are already free and unused. A new wireless short-range optical communication technology that provides connectivity within a local area network, using LEDs to transmit data according to optical light properties,

The features offered by VLC and explain why it is an important alternative to the wireless communication technologies below. the list of outstanding advantages provided by VLC.

• Cost-effectiveness

• Energy efficiency

• Unorganized large bandwidth

Today, RF technology is mature. However, the LED lamps used in VLC are also used for lighting. Therefore, the exact price is lower. The lamps used in VLC are highly efficient devices that use 75% less energy and 25 times longer than incandescent lighting. Because the energy used by LEDs is essential for lighting, the VLC is very energy efficient. The United States estimates that the most considerable possible improvement in energy savings will be achieved in the widespread use of LED lighting. According to these estimates, the extensive use of LEDs by 2027 could save about 348 TWh of

electricity compared to non-use of LED. This is a large amount of energy-saving equal to the annual electricity production of 44 large power plants.

Many researchers have focused deeply on communication science through visible light. Several positioning methods have been developed to support communication through visible light [19]. This technique is based on the use of a matrix of optical sensors or a combination of image sensors. The weak performance of this method lies in the high cost of its construction, accompanied by a slow transfer of data during communication. RSS is the best of these methods in terms of relatively low cost as well as the simplicity of their physical and software requirements [20]. This method requires pre-calibration in terms of the location of the ID, in addition to evaluating the variables. Despite the calibration procedures, it is possible to conduct a location with only two dimensions [21]. In this work, NNCEA is proposed to calculate the location using the traditional RSS percentage as an input. The proposed algorithm uses calculated coordinates for light receptors from LEDs using relative RSS value to produce a more accurate and stable localization. The results obtained indicate that the accuracy of positioning is better regardless of how the sources are arranged and the pattern of their radiation. To achieve high-speed connectivity, Optical Frequency Division Multiplex (OFDM) is widely used in the RF system. Recently, some work suggests that OFDM is also an effective means of optical wireless communication (OWC) after some improvements to modulation / direct detection modulation (IM / DD) [22]. The Channel equalization is a frequent attribute in the VLC field. As mentioned in [23], the LED modulation bandwidth is affected by several complex factors. Thus, a more powerful tie is critical to VLC. Settlement methods can be classified into two categories, the frequency domain

equalization (FDE) and time-domain equalization (TDE). Traditional FDE consists of some pilot-supported methods such as interpolation [24] and compressive sensing (CS) [25]. While TDE methods include decision-directed least mean square (DDLMS) [26], More recently, machine learning (ML) has been actively investigated for its applications in channel estimation of the RF system [27]. In VLC, there are also some successful schemas. Rajbahandari et al. Proposition of a hybrid artificial neural network matrix (ANN) to modify the on-off keying (OOK) based OWC system [28]. Lee et al. Provide an AE-based transmitter and receiver using color modulation techniques such as color shift keying (CSK) [29], and color intensity modulation(CIM). All ML-based reconciliation methods for VLC have not yet covered OFDM. Besides, the New Linear Neural Network System (NLNNS) that possesses a stronger expression capacity than the normal ANN is not explored in the VLC domain. We choose DFTS-OFDM as modem schema. Neural Network System for Proposed Equalization Personnel (NNS) which includes New linear neural network circumference (NLNNS) and a full layer (FL). When the signal-to-noise ratio (SNR) is 30 dB and the 16/32/64 (QAM) quadratic capacity adjustment, the original BER is about 0.5 while the BER after recovery is 10^{-5}. Also, we select the OMP [30] algorithm for comparison. Numerical simulations also justify that the performance of BER for our equalizer outweighs conventional methods.

A new suggested method in [31] , overlapping the time range to achieve the same spectral efficiency as DCO-OFDM for both U-OFDM and ACO-OFDM. In recent times, MIMO, and index modulation communication methods have been attracted substantial consideration in the VLC literature filed for additional bits transfer with low power consumption. In [31], MIMO-

VLC-based systems are look over for multi-user status. Index-modulation procedures, which use the building blocks of the communications systems, are designed to transmit additional bits of information, especially promising in efficient IM / DD applications in energy and spectrum use. Index-based transmission systems provide extra freedom to compensate for phase loss [33]. Spatial-modulation (SM), which is proposed in [34], is the most common form of index modification, was adopted for MIMO-VLC systems.

2.2 Literature Survey

In 2007 J. Grubor et al. [35] discuss the response time of the mixed LED which is much higher than the time of the phosphorus response because the frequency modulation is limited to a few MHz, although the white phosphorus white is low in cost.

In 2011 Kwonhyung Lee et al. [36] discuss the dispersion properties within multiple VLC paths by simulating the computer to compare VLC's energy-delay profile with that of infrared communications. It was concluded that the total received the power of the reflected paths and the RMS delay spread for VLC cases were smaller than those in the cases Infrared, which means that VLC has a larger optical transmission bandwidth, for multiple optical sources, the channel bandwidth is limited in some environments due to strong LOS components.

In 2013 W. Zhang et al. [37] discuss many attractive indoor solutions based on radio wave technologies, including cellular devices, Bluetooth, UWB, WLAN, RFID, etc. These methods verify positioning accuracy from tens of centimeters to several meters.

In 2013 z. Ghassemlooy et al. [38] discuss an indoor non-directed line of sight optical wireless communication (NLOS-OWC) system . first derive the optimized Lambertian order (OLO) expression from the traditional Lambertian LED model. OLO was extracted for specific internal OWC configuration, and in particular, we analyzed the performance of single-cell and four-cell systems using the optimal Lambertian and non-optimal commands. The characteristics of the channel, including the distribution of optical receiving power and multipath propagation, were simulated and analyzed. The results presented show that the received optical power and bandwidth can be improved by adopting Lambertian order (LO) optimization. While this optimization factor depends on the room dimension and the number of cells, it is more critical for multicellular internal configurations.

In 2013 J.J. Tan et al. [39] discuss a simplified IR and FR method of the MIMO internal optical wireless communication channel using the white LED. The beam tracking method is provided to estimate the impulse response (IR) and frequency response (FR) according to the number of reflections, limiting the reflections within three times. The IR and FR are connected to the LED transmitter layout and receiver position. If we repair the transmitters, the impulse response and frequency response varies depending on the location of the receiver. Also, simulation results show that future performance in the central chamber is better than near-future performance. The reflection channel bandwidth is related to reflection times. For a direct response to the broadest range, the R1 has the widest bandwidth of 25 MHz, R3 has bandwidth 12 MHz.

In 2014 Weizhi Zhang et al. [40] discuss asynchronous internal positioning system based on VLC technology, where the use of the Basic Framed Slotted Aloha (BFSA) protocol as a solution to the problem of multi-channel access. After analyzing the noise of internal environments with direct and indirect exposure to sunlight, it was found that the indoor positioning service was up to 95% accuracy at 17.25 cm assuming direct exposure to sunlight and accuracy of 95% at 11.2 cm when assuming indirect exposure to sunlight, taking into account the possible faulty positions of the LED lamps and future direction angle.

In 2015 P. H. Pathak et al. [41] discuss mainly two types of visible LEDs. One type is white LEDs that engage much attention like illumination devices. The other type is single color LEDs, like red (R) LEDs that the wavelength emits around 650 nm, green (G) LEDs emits 525nm and blue (B) LEDs emits 470 nm. Usually, LED lights are emitted in red, green or blue from a narrow spectral range, according to the material system. The two technologies to generate white light by using LEDs are one technology. It creates white phosphorescent LEDs that are the most popular types of the white LEDs currently used. This type of white light is constructed using a blue LED, which has a yellow phosphorus coating on the package. When the power flows into the LED chip, the blue light is emitted, and part of it is absorbed by the phosphorus to generate a yellow-yellow light. Blending the blue lights and the yellow lights leads to a combination that creates white light. White lights of different colors and temperatures are produced by adjusting the thickness of the phosphorus layer.

In 2015 Liang Wu et al. [42] discuss an in-depth analysis of the adaptive spectral efficiency of the adaptive adjustment of three different high-speed

VLC schemes: DC-biased optical OFDM (DCO-OFDM), OFDM and the equivalent of single-carrier frequency (SC-FDE) In the low-signal-to-noise ratio area, and the asymmetrically clipped optical OFDM (ACO-OFDM) adaptive modulation system is superior to other planners. The SC-FDE adaptive adjustment achieves better performance than the DCO-OFDM-based schema, which is much simpler than the other planners. The complexity of removing the SC-FDE diagram formation is less than the complexity of OFDM-based schemas, because SC-FDE uses the same modulation scheme one frame, while OFDM-based schemas use different formation schemes for different sub-carriers.

In 2015 Yingjun Zhou et al. [43] discuss The VLC Positioning System is based on LEDs that combine MIMO technology with diversity reception technology and demonstrated that the use of diversity reception technology would have a positive effect on receiving performance. Also, the best reception area and lamp spacing and half the half-angle of power and the distance between two receptors can be useful Very practical.

In 2015 Tran The Son et al. [44] discuss a new model of adaptive correction to recover 4 × 4 MIMO VLC data in the case of missing pilot signals from transmitters. The well-known trigonometric technique was introduced with receptor knowledge of user locations to predict the current site. The results showed that data transmission across the four channels received a free error, providing MIMO VLC links more smoothly and better than other proposed models.

In 2015 Cuiwei He et.al[45] discuss Analysis of photoreceptor performance by using optical detector (PD) with two different fields of view (FOVs) in a MIMO optical wireless communication system that used IM/DD,

Comparisons between the receiver FOV-1 and the FOV-2 receiver for both MIMO 4 × 4 and 6 × 4. The new side is that the PD devices on the receiver do not all have the same FOV. The new aspect is that the PD devices on the receiver do not all have the same FOV. The use of PDS with different FOVs leads to a reversible channel matrix even when the PDs are spaced up close. The channel matrices are calculated as a function of the receiver position. These calculations show that the channel matrices are fully arranged for the eight versions of PD for each of the receiver types for all received locations. Also, the properties of the channel matrix of the FOV-2 receiver lead to a higher signal to noise ratio (SNR) at the output of the linear equations because the channel matrix elements of the FOV receiver are very similar, and the equation results in a significant noise improvement. The FOV-2 receiver overcomes this problem because PDS with the smaller FOV produces zero elements in the channel matrix when the sender is assigned out of FOVs. As a result, a minimum signal-to-noise ratio (SNR) can be achieved with a much smaller receiver when using a FOV-2structure. The BER distribution of the MIMO system has also been studied using linear equations ACO-OFDM, ZF, and MMSE. The BER distribution as a position function in a typical room shows that higher BER rates are obtained when the receiver is near the center or corners of the room.

In 2017 Anil Yesilkaya et al. [46] discuss a new way to circulate LED index modulation method fort MIMO-OFDM-based VLC systems. This is achieved by multiplexing exploitation along with the LED index modulation. So the real and the imaginary components of OFDM signals are separated from the complex time-domain first, and then the resulting bipolar signals are transmitted via the VLC channel by encrypting the signal information in the LED indexes where The first scheme is based on the flat frequency channels

and the second in the selective frequency channels. It is concluded from the computer simulation that the performance of the BER for the VLC system of the second designer is not significantly affected by the frequency selection of the channel while maintaining its advantages in spectral efficiency on other MIMO-OFDM.

In 2017 Syifaul Fuada et al. [47] discuss the investigation of the receptor characteristics of many commercially available photovoltaic VLCs with the Los channel. The results showed that the field of view (FOV) does not affect the character of the receiving power if the (n factor) refractive index is ignored. This can be seen in the first case that half the angle of the transmitter is changed. In case II, by changing the power of LED and mode III, by changing the channel distances to which d (in meters) are indicated. It is known that factor n plays an important role in significantly improving the receiving capacity in the photovoltaic diode.

In 2017 Yunlu Wang et al. [48] discussed the resource allocation (RA) problem in Li-Fi OFDMA systems, and propose an RA-based optimization scheme and an RA-based randomized scheme. The results of these two schemes are evaluated in terms of computational complexity, data rate, and user integrity, compared with a standard RA schema in the TDMA system. Three results were first extracted as a result of the RA schemes in OFDMA systems superior to their TDMA counterparts in terms of data rate and user integrity due to use Efficient, high-frequency resources, and secondly the result of a low-complexity RA scheme capable of achieving near-optimal performance by reducing 90% of the computational complexity. The last large modification bandwidth may reduce the user data rate with increased non-user bandwidth on the first subcarrier, is not effective for total bandwidth.

In 2017 Mustafa Al-Nassrawi et al. [49] discuss a new way of estimating the receptor position in the VLC system, where it works to place it in a single channel or MIMO VLC system using minimum transmitters. The method is based on estimating user speed between past and current positions. The estimated speed and the received signal strength (RSSI) are obtained from a single transmitter to determine the location of the user compared to current positioning methods such as triangulation. In MIMO VLC, the model for the self-debugging schema will be used to complete the channel status information matrix with missing elements during the experimental signal period. The simulation results show that the method is effective in obtaining the user's position.

In 2018 Kristina Gligori´ et al. [50] discussed the method of internal positioning based on VLC using the compressed sensor. Itis considered that a large number of LEDs transmit their position information and the user's device with a photo-diode. By posing the problem of separating the LED signal in an equivalent compressed sensor frame on the detection of nearby LED lamps using scattered signal recovery algorithms using a proximity method. If the signal separation is possible, the light beam interference regions reduce the fault of the location due to a large number of reference signals, thus comparing the accuracy of the positioning with the error Set the minimum for the proximity method, for different system parameters.

In 2018 Chun Lin et al. [51] Use a method for Visible Light Positioning System depends on backpropagation artificial neural network (BP-ANN) and optical camera connections(OCC), where the position of the receiver is estimated with approximate accuracy based on the encoded cluster coordinates and the typical backpropagation ANN(BP-ANN), respectively.

The results illustrate that the proposed scheme provides an average positioning error of 1.49 cm.

In 2018 Sheng Zhang et al. [52] discuss an internal 3D VLP system that uses RSS ratio measurements with NNPE. The NNPE system provides high-resolution 3D positioning features without knowing the coordinates of LED transmitters and the irradiation model, and results show an average positioning error of less than 5 cm in a coverage area 0.8 x 0.8 square meters with a maximum height of 2 meters from the ceiling.

In 2018 N. Lorri`ere Aix Marseille Univ et al. [53] discuss the performance of the Li-Fi obtained from the OFDM-based Li-Fi test using various photovoltaic modules as photodetectors. Li-Fi was tested and validated compared to CEA-Leti. The DCO-OFDM modification scheme was selected for system configuration under the same conditions as Li-Fi data transfers.

In 2018 Kabiru O. Akande et al. [54] discuss the low-complex detection schemes in Multiple-input, multiple-output conventional carrier less amplitude, and phase (MIMO CAP)and compare their performance with optimal ML detector performance. The ordered successive interference cancellation (OSIC), Zero-forcing ordered successive interference cancellation (ZF-OSIC), and minimum mean square error detection with optimally-ordered successive interference cancellation (MMSE-OSIC)detection schemes were found to provide a significant improvement in performance on the corresponding linear detection devices, ZF and MMSE. Also, MMSE-OSIC was found to outperform ZF-OSIC by gaining 1.5 dB on Calculates a few additional calculations, and MMSE-OSIC requires only an increase of 5 dB SNR per bit compared to the non-practical Maximum Likelihood (ML) detector. MMSE-OSIC concluded the best detection system

from the ML detection system in terms of comparing the performance complexity of the MIMO CAP system.

In 2018 Chen Chen et al. [55] discuss a new non-orthogonal multiple access technique (NOMA) to improve the rate of attainment of MIMO systems, to ensure efficient and efficient power distribution in MIMO-NOMA-based internal VLC systems with low computational complexity. The normalized gain difference power allocation (NGDPA) method was proposed by exploiting user channel conditions. The results were created in a 2 × 2 MIMO-VLC internal system, NOMA with NGDPA achieves a significantly improved rate compared to NOMA with GRPA. A growth rate of 29.1% can be achieved by using NOMA with NGDPA in the 2 × 2 MIMO-VLC system with three users.

In 2019 Rui Bian et al. [56] discuss the VLC system has a data rate of 15.73 Gb / s after applying the forward error correction (FEC) on a 1.6 m link. The Wavelength-division multiplexing (WDM) system is designed with four wavelengths of visible light based on double-color mirrors, and each wavelength is formative using DCO- OFDM With adaptive bit loading, and optimally optimized system parameters, a data transfer rate of 15.73 Gbit / s is achieved with a BER below the HDFEC limit of 7% which is 3.8×10^{-3} on a wireless link 1.6 meters.

In 2019 Mohammad Dehghani Soltani et al. [57] discuss the probability density function (PDF) derivation of SNR for randomized devices, based on the derived PDF where the BER performance of DCO-OFDM in the AWGN channel is evaluated with random-guided User Equipment (UEs). The average BER is roughly rounded at random and exactly matches With the exact criterion and thus investigate the role of the CE angle that ensures the presence of the LOS link in the UE FOV. Also, the great effect of the optimal

bias towards the access point on the BER performance is investigated. The impact of random direction on the mean signal to interference ratio and noise (SINR) in a multiple access point scenario (AP).

The brief description of previous researches is shown in table 2.1.

Table-2.1 Summary of Literature Review

No	Year	Researcher	Method
1	2014	Weizhi Zhang,et.al	Use method asynchronous internal positioning system based on VLC technology. Where the use of the BFSA protocol as a solution to the problem of multi-channel access. after analyzing the noise of internal environments with direct and indirect exposure to sunlight, the results found that the indoor positioning service was up to 95% accuracy at 17.25 cm assuming direct exposure to sunlight and accuracy of 95% at 11.2 cm when assuming indirect exposure to sunlight

2	2015	Yingjun Zhou ,et.al	Use a method for The VLC Positioning System is based on LEDs that combine MIMO technology with diversity reception technology and demonstrated that the use of diversity reception technology would have a positive effect on receiving performance. Also, the best reception area and lamp spacing and half the half-angle of power and the distance between two receptors can be useful Very practical.
3	2015	Tran The Son , et.al	A new model of adaptive correction to recover 4 × 4 MIMO VLC data in the case of missing pilot signals from transmitters. The well-known trigonometric technique was introduced with receptor knowledge of user locations to predict the current site. The results showed that data transmission across the four channels received a free error, providing MIMO VLC links more smoothly and better than other proposed models
4	2017	Anil Yesilkaya, et.al	A new way to circulate LED index modulation method fort MIMO-OFDM-based VLC systems. This is achieved by multiplexing exploitation along with the LED index modulation.

5	2017	Syifaul Fuada	Method for the investigation of the receptor characteristics of many commercially available photovoltaic VLCs with the Los channel. The results showed that the field of view (FOV) does not affect the character of the receiving power if the (n factor) refractive index is ignored.
6	2018	Kristina Gligori´	The method of internal positioning based on VLC using the compressed sensor. It considered that a large number of LEDs transmit their position information and the user's device with a photo-diode.
7	2018	Sheng Zhang	an internal 3D VLP system that uses RSS ratio measurements with NNPE, the NNPE system provides high-resolution 3D positioning features without knowing the coordinates of LED transmitters and the irradiation model.
8	2018	Chun Lin,	Using a method for Visible Light Positioning System depends on artificial neural network (ANN) and optical camera connections.

9	2018	Kabiru-O. Akande,	Using the low-complex detection schemes in Multiple-input multiple-output carrier less amplitude, and phase (MIMO CAP)and compare their performance with optimal ML detector performance. The OSIC, ZF-OSIC, and MMSE-OSIC detection schemes were found to provide a significant improvement in performance on the corresponding linear detection devices, ZF and MMSE.

CHAPTER THREE

Methodology

3.1 Method Outline

In this method the work was divided into two parts. The first part is a new algorithm called Neural Network Coordinate Evaluator Algorithm (NNCEA) to determine the exact location user, while the second part is a new algorithm called New Line Neural Network System (NLNNS) in channel coding to make work multi-input multi-output (MIMO**).** This is done using a modern software package (Matlab R2013a).

3.2 Positioning using NNCEA Algorithm

The proposed positioning system is shown in Fig. 3.1(a) considers the origin point of the coordinate placed in the center of room ,which means dividing the room to four sectors and indicating the sources of LEDs as L1(x=-2,y=2), L2(x=2,y=2), L3 (x=-2,y=-2) and L4 (x=2,y=-2) where the L is the position of LED, x is the length, y is the width and the recipient is referred to as P. The four optical sources are distributed on the roof of the room. The optical receiver is under the scope of the sources. Each source independently operates a different sinusoidal frequency signal. The received signals are first processed using the Least Mean Square (LMS) filter algorithm and then using the Receive Signal Strength (RSS) percentage estimator, finally sent to the proposed NNCEA as shown in Fig 3.1(b) . An algorithm to calculate the location, as shown in the appendix A1.

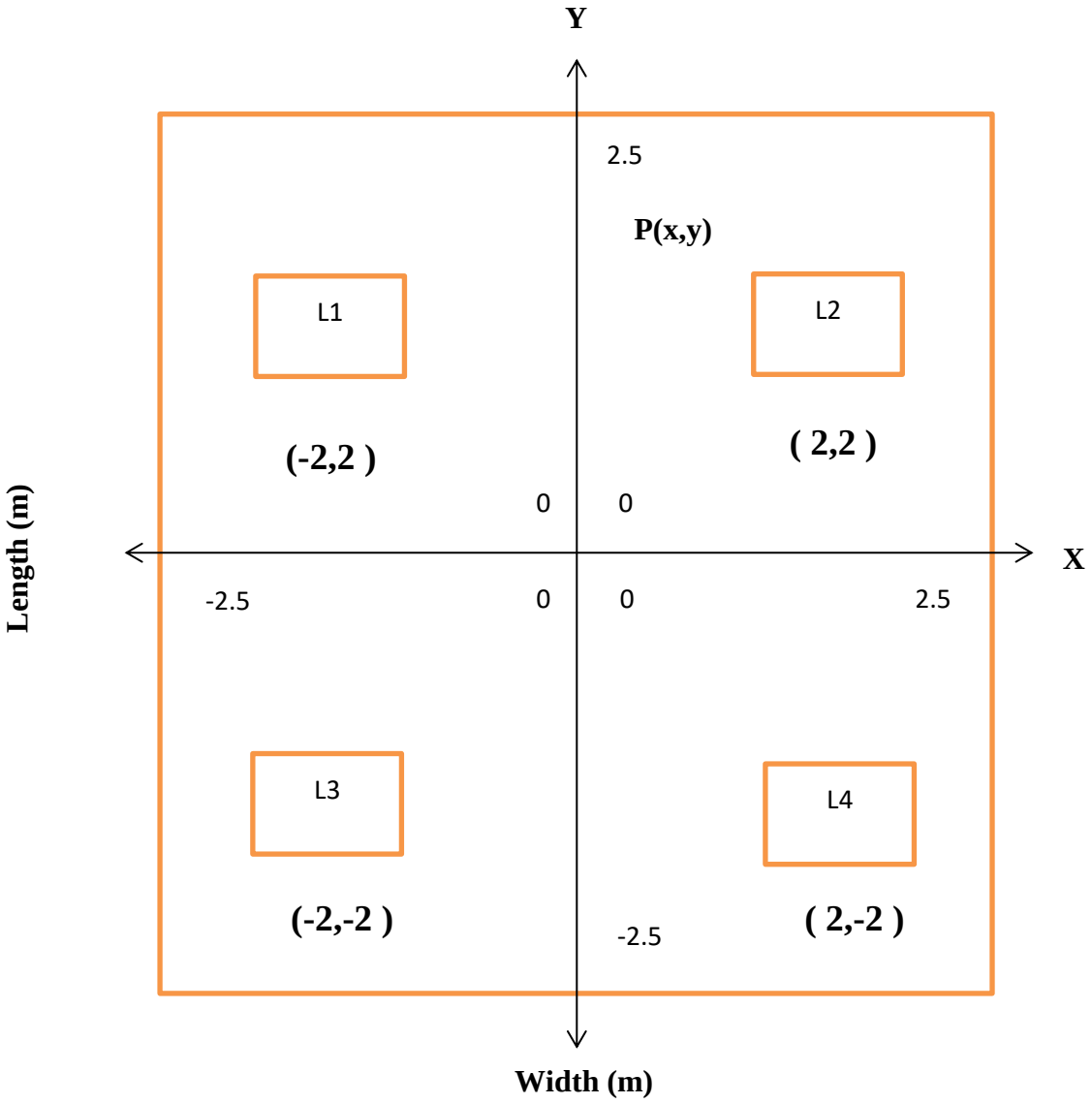

Figure 3.1(a) Schematic of the proposed system NNCEA

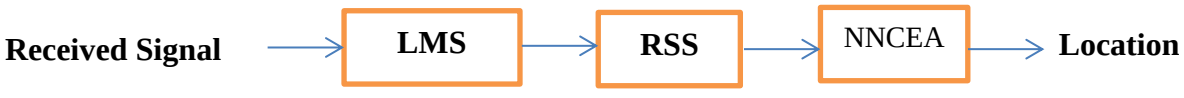

Figure 3.1(b) Block diagram of the proposed system NNCEA

3.2.1 NNCEA Performance

A 3D positioning system X, Y, Z are calculated for the receiver p(x,y), as shown in Fig. 3.1,(Note: Z is fixed as Z=0.5m) based on the RSS percentage values extracted from the four primary sources. An intermediate layer, which composed of 5 neurons within the hidden layer is used to encode their bases coded as b_{1n} and in line with the T_{mn} encoded weights of the m-input of the n-neuron, while the T_{np} is used to represent the weight of the p-output of the m-neuron. The b_{2p} is then assigned to the exits as a partial adjustment, f is the cost function of the activation. The algorithm can be stated as in equation 1:

$$\mathbf{L_p = f\left(\sum_{n=1}^{5} T_{np}\left(f\left(\sum_{m=1}^{3} T_{mn}\, Y_m\right) + b_{1n}\right) + b_{2p}\right).} \qquad \mathbf{(3.1)}$$

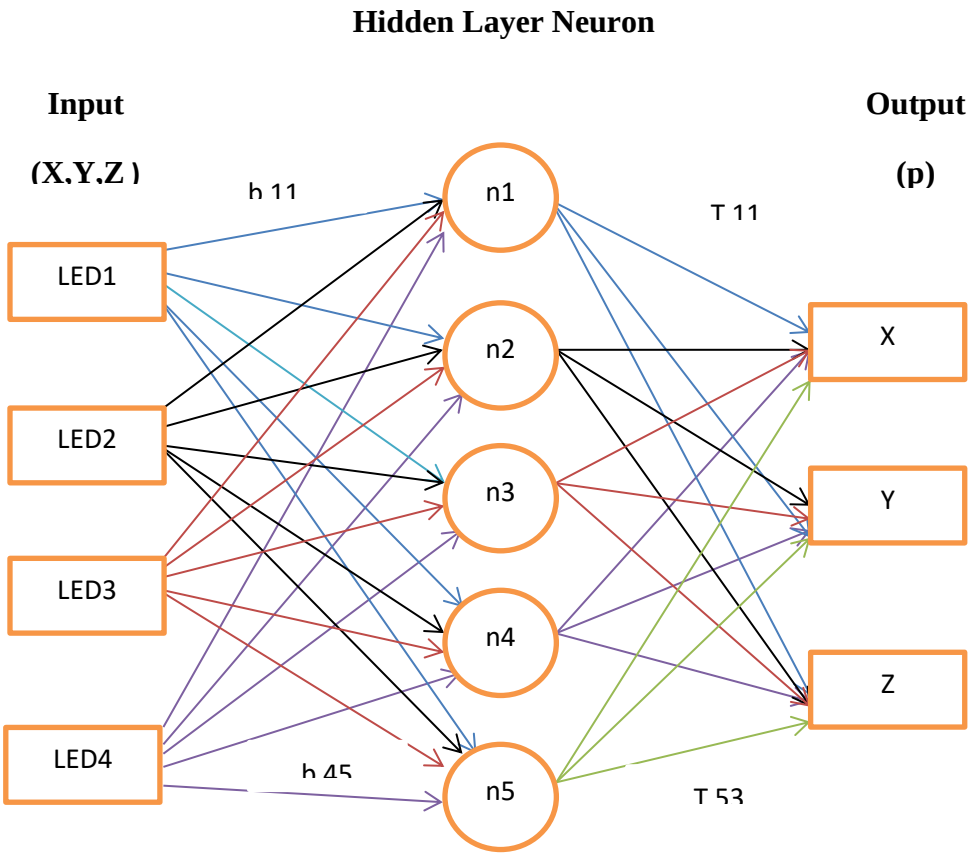

Fig.3.2 The single-layer neural network positioning system.

The step before applying the proposed system is to do system training NNCEA using pre-fixed and pre-defined positions, using back-propagation technique [58].

From a practical point of view, LEDs light radiation is a time-varying power signal, due to the power-supply fluctuation, and the continued changing of the temperature. The fluctuated power, due to unstable LED-intensity, results in time-variant RSS values, which produces a time-varying positioning evaluation. To override this problem, a modified-quantity of RSS is calculated. This procedure tack in account three contiguous LED Lamps in each step to evaluate the positioning. The modified input ratio of the RSS will be:

$$\boldsymbol{RPs_m} = \frac{(Rs_{m+1} + Rs_{m-1})/2}{Rs_m}$$

$$= \frac{\{(i_{m+1}+1)cos^{i_{m+1}+1}(\theta_{m+1})id^2\}+\{(i_{m-1}+1)cos^{i_{m-1}+1}(\theta_{m-1})id^2\}/2}{(i_m+1)cos^{i_m+1}(\theta_m)(id+1)^2(id-1)^2} \boldsymbol{R12} \qquad \textbf{(3.2)}$$

$$\boldsymbol{R_{12}} = \frac{R_{m+1}+R_{m-1}}{2} \qquad \textbf{(3.3)}$$

Where R_{m+1} represents the proportion of light intensity between LEDs m and m+1 in order, as well as R_{m-1} is the rate of light intensity between LEDs m and m-1 respectively (m=1, 2, 3), id distance from the LED to the receiver. So, the impact of the unbalanced intensity of the Lamps is minimized.

3.3 Principle of Optimization

As a first step, the transmitted power of data communications will be calculated at different LED sites to achieve a uniform distribution of signal-to-noise ratio(SNR) at the receiver plane.

The receiving power in channel modeling, SNR, is expressed as one of the most important criteria when discussing system performance will be

discussed in this sub-section. In this work, there are N-LED locations distributed uniformly on the room ceiling. A Lambertian radiation pattern is used for each LED. Also, P receivers are located (0.5 m above the ground) uniformly on the work plane. However, the total received power is given by

$$\boldsymbol{Pr_{Total} = Pr_{los} + Pr_{diff}} \qquad \textbf{(3.4)}$$

The Received power of LOS is given by

$$\boldsymbol{Pr_{los} = P_{LED} \times H_{los}} \qquad \textbf{(3.5)}$$

Where P_{LED} The power emitted by LED (W) and $\boldsymbol{H_{los}}$ is the channel transfer function and is given by

$$\boldsymbol{H_{los} = \frac{ARX}{h_{dist}{}^2} cos(\frac{\theta \times \pi}{180}) \times Ro} \qquad \textbf{(3.6)}$$

Where ARX is the active photodiode area, h_{dist} is the distance between transmitter and receptor, θ is stander value of the incident angle(60^0), and Ro is the Lambertian radiant intensity can be given as shown

$$\boldsymbol{Ro = \frac{m+1}{2\pi} cos\,\varphi^m} \qquad \textbf{(3.7)}$$

Where φ is stander value of the Transmitter Semi-angle (120^0) , and m is the order of Lambertian emission can be given by

$$\boldsymbol{m = \frac{-log\,2}{log\,cos\,\varphi}} \qquad \textbf{(3.8)}$$

The Received power of diffusion is given by

$$\boldsymbol{Pr_{diff} = \frac{P_{LED}/(A_{room}) \times rho}{(1-rho) \times ARX}} \qquad \textbf{(3.9)}$$

Where A_{room} is the Whole room surface area and *rho* is the Average reflectivity. The received power for N-LEDs can be shown as

3.3.1Calculat The indoor channel properties (SNR)

The SNR can be expressed in the photodetector (PD) in a responsible manner, the receiving optical power, and the noise variation as well[59] :

$$\boldsymbol{SNR = \frac{Pr\_total^{2}}{Oemga\ total^{2}}} \qquad \textbf{(3.10)}$$

Where Omega total (σ_T) is the Total noise variance, and it can be given by

$$\boldsymbol{Omega\ total\ (\sigma_T) = \sigma_{shot} + \sigma_{amplifier}} \qquad \textbf{(3.11)}$$

[44], the Shot-noise variance can be given as

$$\boldsymbol{\sigma_{shot} = 2 \times q \times Rr \times (Pr_{Total} + P_{amb}) \times Bn} \qquad \textbf{(3.12)}$$

Where q is the Electron charge**,** Rr is the Photodiode responsivity, and Bn is the noise bandwidth and $P_{amb}$is the ambient light power.

The $\sigma_{amplifier}$ is given by

$$\boldsymbol{\sigma_{amplifier} = I_{amp}^{2} * Ba} \qquad \textbf{(3.13)}$$

Where I_{amp} is the Amplifier noise density and $\boldsymbol{Ba}$ is the Amplifier bandwidth.

The illumination can be expressed in terms of the photodetector (PD) responsibly as well[59] :

$$\boldsymbol{Lamb = \frac{I}{h\_dis^{2}} \times \cos\theta} \qquad \textbf{(3.14)}$$

Where $\boldsymbol{I}$ the luminous intensity in angle, and it can be calculated by:

$$\boldsymbol{I = \frac{I_0}{cos\ \varphi^{m}}} \qquad \textbf{(3.15)}$$

$\mathbf{I_0}$ is the center luminous intensity of an LED.

Some parameters that used in NNCEA algorithm has shown in table 3.1

Table 3.1 Positioning -VLC parameters

Parameters	Value
$\boldsymbol{\varphi}$	φ is the Transmitter Semi-angle (FOV) = 60^0 [46]

θ	θ is the incident angle = 120^0 [46]
Room diminution	$5\times5\times3$ (m^3)
ARX	the photodiode active area = 0.5 (mm)
M	The order of Lambertian
$\mathbf{P_{LED}}$	The power emitted by the LED= 0.02 (W)
Rr	The Photodiode responsivity = 0.55 (A/W)
Ba	The noise bandwidth = $4.5e^6$ (Hz)
$\boldsymbol{P_{amp}}$	The ambient light power.
$\boldsymbol{I_{amp}}$	The Amplifier noise density = $5e^{-12}$ ($A/Hz^{0.5}$)
$\boldsymbol{I_0}$	The center luminous intensity of an LED = 24 (cd)

3.4 OFDM diagram using NLNNS algorithm

To the best of our knowledge, we have used a new block diagram. With M (M is the Modulation order), N_d (N_d is the number of subcarriers), N_f (is the Points of FFT), N_{cp}(N_{cp} is the Length of CP), Fs (Fs is the sample rate), and Ns (Ns is the number of transmitted symbols) to arrange the configuration as shown in fig.3.1 . The number of subcarriers, FFT points, the cyclic prefix length (CP), the sample rate, and the number of symbols will be transmitted, respective.

On the modulation, Hermitianl symmetry ensures that the baseband signals are in a real domain. Given i = 0, 1, ..., Ns-1, the $x_1^{(i)} \ni C^{Nf}$ has a structure [59]:

$$\boldsymbol{x_1^{(i)} = [0, Z_0^{(i)}, Z_1^{(i)}, Z_2^{(i)}, \dots., Z_{Nd-1}^{(i)}, \left(Z_{Nd-1}^{(i)}\right)^*, \dots, Z_0^{(i)}]^T} \qquad \textbf{(3.16)}$$

Where $\left[x_1^{(i)}\right]_0$ and $\left[x_1^{(i)}\right]_{\mathrm{Nf}\,/\,2}$ are assigned Nf / 2 as zeros to remove the DC component. ,, This step is Nd = Nf / 2 - 1.

The $\boldsymbol{x_2^{(i)} \in K^{Nf}}$ They are obtained by

$$\boldsymbol{[x_2^{(i)}]_m = \frac{1}{\sqrt{Nf}} \sum_{n=0}^{Nf-1} [x_1^{(i)}]_n e^{\left(j\frac{2\pi}{Nf} mn\right)}} \qquad \textbf{(3.17)}$$

$$\boldsymbol{= \frac{2}{\sqrt{Nf}} \sum_{n=0}^{Nf/2-1} K[x_1^{(i)}]_n e^{\left(j\frac{2\pi}{Nf} mn\right)}} \qquad \textbf{(3.18)}$$

Where *K* is the pure rate of the system and *m* is the minimum-batch Size. At the same time, the original signal is expressed in the training package by $\boldsymbol{X_2 = \left[x_2^0, x_2^1, x_2^2, \dots x_2^{(Ns-1)}\right] \in K^{Nf \times Ns}}$ **,** the normalize $\boldsymbol{X_2}$ the interval must be [−1, 1] to alleviate the phasing problem of fading in the training stage.

$$\boldsymbol{K = M \times \frac{N_d}{N_f} \times F_s} \qquad \textbf{(3.19)}$$

Finally, an x signal to transmit after the introducing of CP along Ncp at each $\boldsymbol{x_2^{(i)}}$. Given the impulse *h* and noise added *n*, the received signal *y* is

$$\boldsymbol{y = (x \times h) + n} \qquad \textbf{(3.20)}$$

In the side of the demodulation, we get the $\boldsymbol{y_1^{(i)} \in K^{N_f}}$ after removing CP, $Y_1 = [y_1^{(0)}, y_1^{(1)}, y_1^{(2)}, \dots y_1^{(N_s-1)}] \in K^{N_f \times N_s}$.

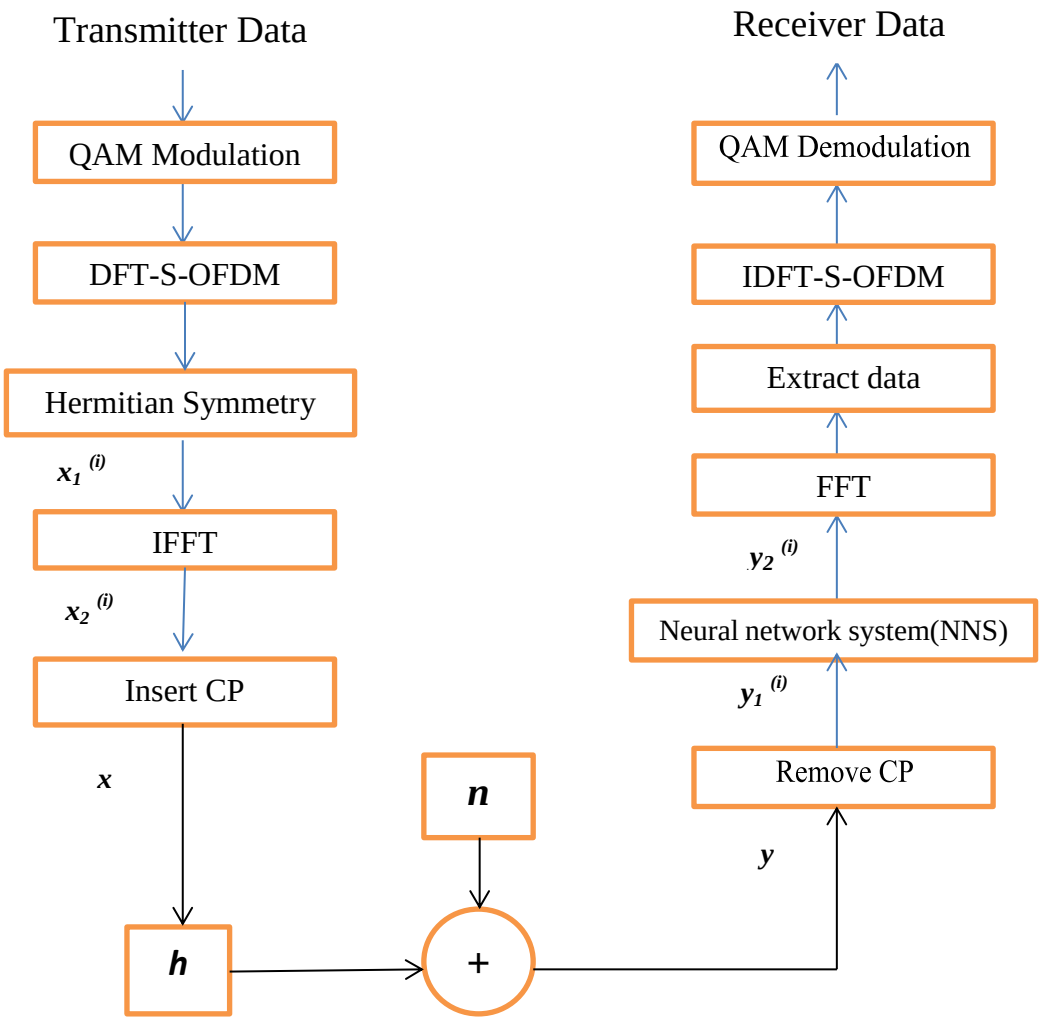

Fig.3.3 System Model Transmitter and Receiver

Fig (3.3) illustrate the structure of the Transmitter and Receiver system The transmitter consists of five-stage while the receiver consists of six-stage.

In the transmitter side, the data transmitted entered to the first stage, which is QAM-Modulation to modulate the signal with modulation index (M=4,8,16). The next stage is the Discrete Fourier Transform – Spread –OFDM (DFT-S-OFDM) that used to operate in a real-time signal sample. After that, the signal

entered to third stage, which is Hermitian symmetry to ensure the baseband signals are in real domain. The fourth stage that signal entered is Inverse Fast Fourier Transform(IFFT) to convert from Frequency-domain to Time-domain. The last stage is Insert Cyclic Prefix (insert CP) used as a header to eliminate multiple paths by making channel estimation easy. Finally, the output signal from the last stage multiply by Impulse response (h) and additive with noise (n) to produce the data transmitted (y).

In the receiver side, the received signal entered to the first stage which is Remove Cyclic Prefix (Remove CP),then the signal entered to the second stage which is Neural Network System(NNS) for training the signal .the the third stage represents the Fast Fourier Transform(FFT) to convert from Time-domain to Frequency- domain and the stage Extract data used to extract signal from noise. The five-stage represent Inverse Discrete Fourier Transform – Spread –OFDM(IDFT-S-OFDM). The last stage is QAM-demodulation, and the output signal from the last stage represents the received signal.

3.4. 1 Neural network System (NNS)

Figure (3.4) explains the NNS structure that consists of one output layer and two full-layer, where second Full-layer (FL) has no activation function. Common non-linear activation functions include rectified linear unit (RLU), softmax, sigmoid, hyperbolic tangent (tanh(x)), etc. Because there are negative values in NNS outputs, so we select tanh(x) as an activation function with a set of (-1, 1). tanh(x) and its derivatives are expressed, concerned, as

$$\boldsymbol{R = tanh(x) = \frac{e^{x}-e^{-x}}{e^{x}+e^{-x}}} \qquad \textbf{(3.21)}$$

$$\boldsymbol{\frac{dR}{dx} = 1 - (R)^{2}} \qquad \textbf{(3.22)}$$

One of the NLNNS features is to map the original data to a higher dimension. where L1 denotes the length of the filter, C represents the number of channels, W_1 is the Wight $W_1 \in K^{L_1 \times C}$ and the bias added is $b_1 \in K^C$. The NLNNS output can be written as :

$$(\boldsymbol{H_1^{(i)}})_{\boldsymbol{p}} = \boldsymbol{f}((\boldsymbol{W_1})_{\boldsymbol{p}} * \boldsymbol{y_1^{(i)}} + [\boldsymbol{b_1}]_{\boldsymbol{p}}) \qquad \textbf{(3.23)}$$

Where P = 0, 1, 2,..., C - 1 and $H_1^{(i)} \in K^{N_f \times C}$. The $(H_1^{(i)})_p$ Is the result of channel p. It is significant to note that we usually put $\boldsymbol{y_1^{(i)}}$ with zeros so that $(\boldsymbol{H_1^{(i)}})_{\boldsymbol{p}}$ is the same length as $\boldsymbol{y_1^{(i)}}$. Then, we reorder $\boldsymbol{H_1^{(i)}}$ to a new vector

$$\boldsymbol{h_2^{(i)}} = [(\boldsymbol{H_1^{(i)}})_{\boldsymbol{0}}^{\boldsymbol{T}}, (\boldsymbol{H_1^{(i)}})_{\boldsymbol{1}}^{\boldsymbol{T}}, (\boldsymbol{H_1^{(i)}})_{\boldsymbol{2}}^{\boldsymbol{T}}, \dots, (\boldsymbol{H_1^{(i)}})_{\boldsymbol{C-1}}^{\boldsymbol{T}}]^{\boldsymbol{T}} \qquad \textbf{(3.24)}$$

Where $h_2^{(i)} \in K^{CN_f}$, then $W_2 \in K^{CN_f \times CN_f}$ and $b_2 \in K^{CN_f}$, $\boldsymbol{h_2^{(i)}}$ They are processed by

$$\boldsymbol{V_2^{(i)}} = \boldsymbol{W_2 h_2^{(i)}} + \boldsymbol{b_2} \qquad \textbf{(3.25)}$$

$$\boldsymbol{h_3^{(i)}} = \boldsymbol{f}(\boldsymbol{V_2^{(i)}}) \qquad \textbf{(3.26)}$$

Where $V_2^{(i)}$ is pre-activate the first FL and $V_2^{(i)}$, $h_3^{(i)} \in K^{CN_f}$. Finally, the OFDM signal recovery is

$$\boldsymbol{y_2^{(i)}} = \boldsymbol{W_3 h_3^{(i)}} + \boldsymbol{b_3} \qquad \textbf{(3.27)}$$

Where $y_2^{(i)} \in K^{N_f}$, $W_3 \in K^{N_f \times CN_f}$ and $b_3 \in K^{N_f}$. We see that there are N_f and C_{Nf} neurons in the first and second FL, respectively.

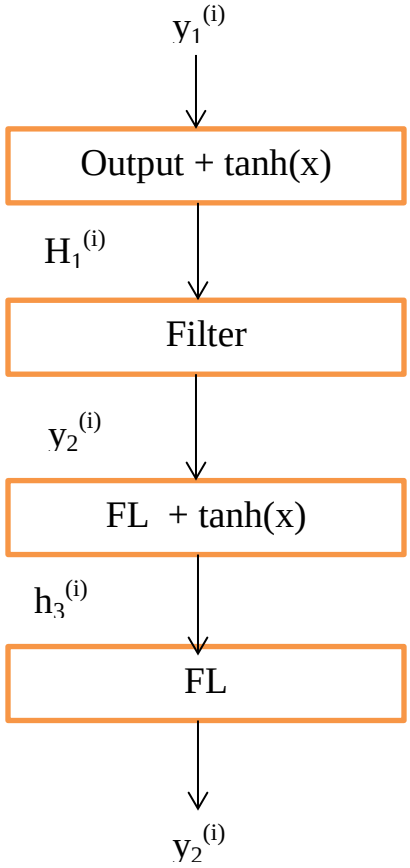

Fig 3.4 Neural network (NNS) details.

3.5 OFDM diagram using NLNNS algorithm for MIMO System

Based on the previous section 3.4 that deals with OFDM system transmitter and receiver , we have developed fig 3.3 by using Separator and estimator to establish Multi Input-Multi Output –OFDM system (MIMO-OFDM).

For MIMO transmission, technology depends on the LED indicator adjustment. After the parallel conversion to serial (P / S), for each time signal OFDM X_q, where q= 0, 1,2,...,N-1 ,First, the real and imaginary parts of the composite signal X_q are separated as $X_q = X_q$, Re + j X_q,Im. after that, the result of real signals, but the bipolar X_q, Re, and X_q, Im are processed by

negative-positive separators (+/-) to obtain the following positive real signals[46]:

$$X_{q,Re}^{+} = \begin{cases} X_{q,Re} & If \quad X_{q,Re} > 0 \\ 0 & If \quad X_{q,Re} < 0 \end{cases} \tag{3.28}$$

$$X_{q,Re}^{-} = \begin{cases} 0 & If \quad X_{q,Re} > 0 \\ -X_{q,Re} & If \quad X_{q,Re} < 0 \end{cases} \tag{3.29}$$

$$X_{q,Im}^{+} = \begin{cases} X_{q,Im} & If \quad X_{q,Im} > 0 \\ 0 & If \quad X_{q,Im} < 0 \end{cases} \tag{3.30}$$

$$X_{q,Im}^{-} = \begin{cases} 0 & If \quad X_{q,Im} > 0 \\ -X_{q,Re} & If \quad X_{q,Im} < 0 \end{cases} \tag{3.31}$$

These signals can be sent simultaneously from the $n_R \times n_T$ MIMO VLC system, where n_R and n_T refer to the number of receiver units (Rx) and transmitters (Tx), respectively. The positive OFDM time samples and the real value $X_{q,Re}^{+}, X_{q,Re}^{-}$, $X_{q,Im}^{+}$ and $X_{q,Im}^{-}$are sent via the optical MIMO channel $n_R \times 4$ for q=0,1,2,…,N-1.so fig 3.5 represented MIMO system model.

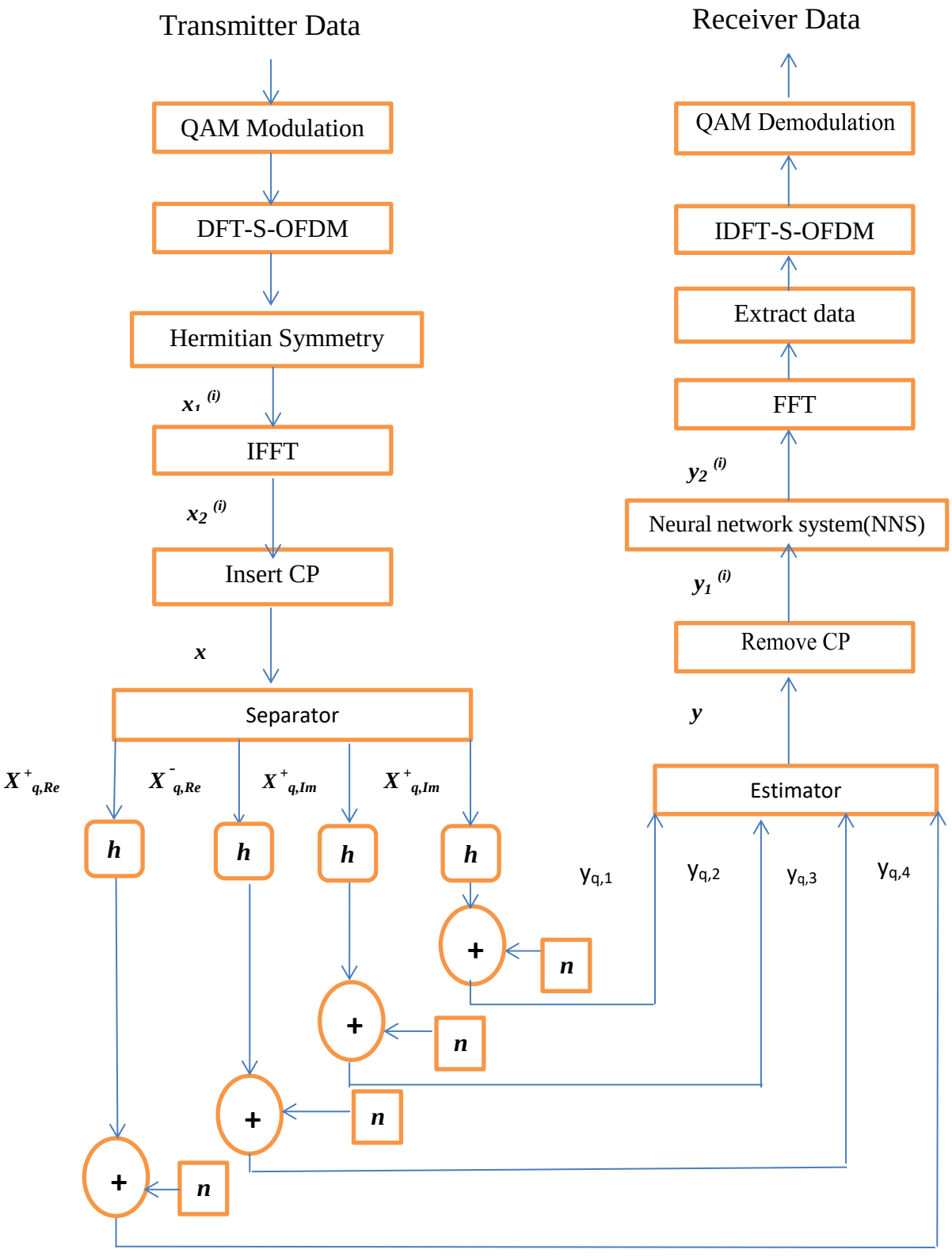

Fig.3.5 MIMO –OFDM system model

Calculates the relationship between SNR and $BER_{RZ\text{-}OOK}$ with the following equation[59]:

$$\boldsymbol{BER_{RZ-OOK} = \frac{1}{2} erfc \frac{1}{2} \sqrt{SNR}} \qquad \textbf{(3.32)}$$

CHAPTER FOUR

Result and Discussion

4.1Result and Discussion

In this chapter, show and discuss the result that obtained it from our method by using simulation Matlab R2013a.

4.2 Positioning using NNCEA

The LEDs are located at the room ceiling with coordinates of L1 (2, 2), L2 (-2, -2), L3 (2, -2), L4 (-2, 2) which are shown in chapter three fig 3.1. The room is divided into 121 different positions are calculated by using eq.(3.1) that applying in simulation Matlab. The span between any adjacent Positions is 0.5m. The RSS has high oscillation, which is maybe produced by the instability of the power source, while the RSS ratio remains highly steady.

The plot of the locating error of the proposed NNCEA using RSS percentage has shown in fig (4.1). However, the NNCEA using RSS percentage outperforms the one directly RSS amounts. The average positioning error is too small for an indoor positioning system, at a first sector area ($5\times5\times3$ m^3) of the testing room. The RSS values can be affected by the walls and furniture that did not take into account in this work. A multi-path effect can be caused by these factors, as well as a dispersion in the signal, which means an error in positioning. Suitable parameters selection leads to minimizing the positioning error. As shown in fig (4.1), a tolerable error caused by the above factors is produced.

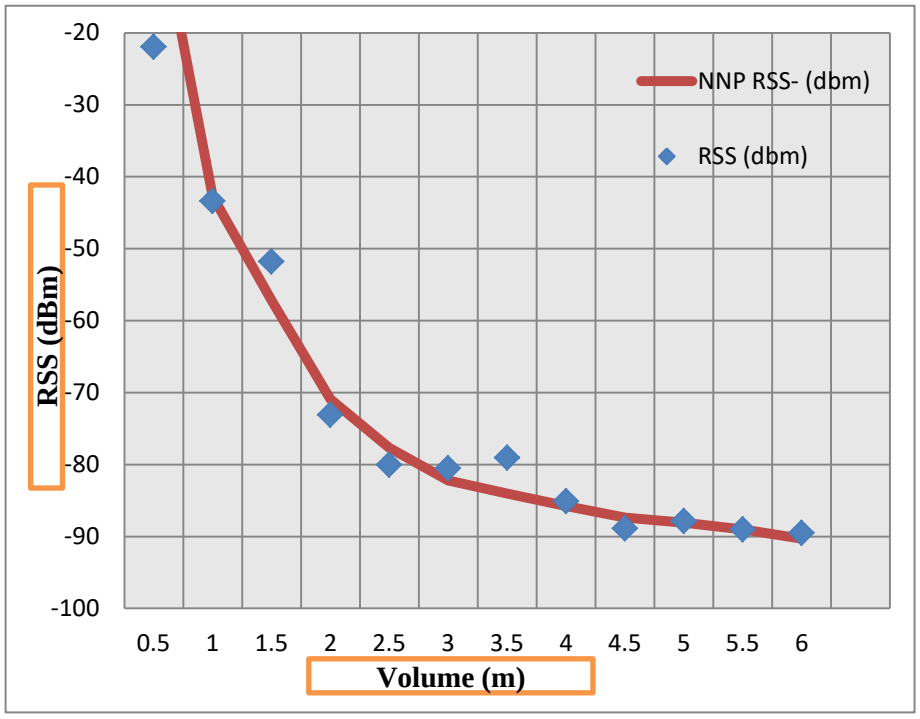

Figure 4. 1 The plot of positioning error of NNCEA using RSS percentage.

According to our Results, we enhancements the accuracy of the site calculation from 10 to 15 cm as well as improved positioning accuracy outside the cell and this is lead to enhance data rate,

4.2.1 SNR and Received Power

Figure (4.2), illustrate the value of the received power at the range of $(1.53\times10^{-7}$ -1.59×10^{-7})W for the first quarter at a testing room , where the power received has calculated by using eq.(3.4) which is mention in chapter three. where these value is fairly acceptable depending on the value of SNR in this quarter.

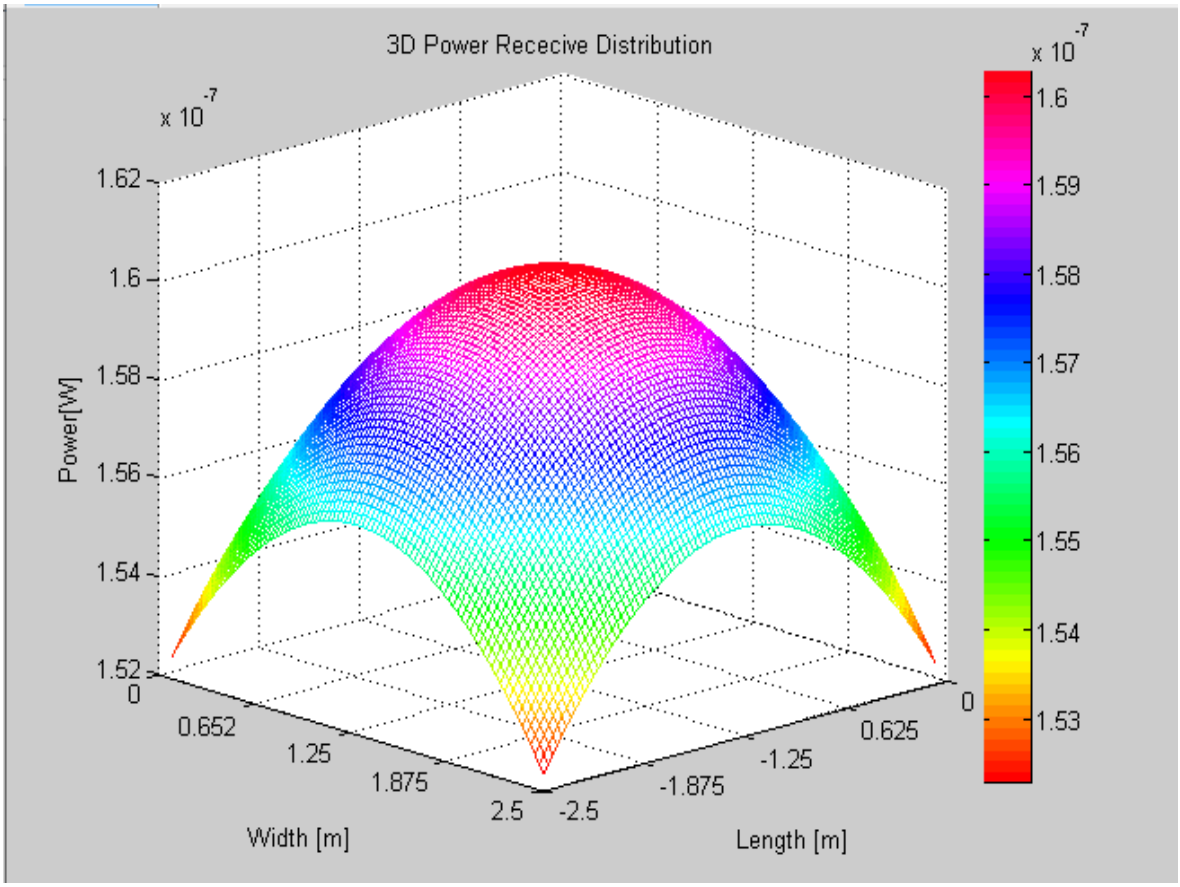

Figure 4.2 A distribution of power receive for the first quarter.

Figure (4.3), illustrate the value of the received power at the range of $(1.11\times10^{-7}$ -1.38×10^{-7})W for the best point in the testing room.

Referring to fig (4.2) a room with dimension $(5 \times 5 \times 3)m^3$ and four LEDs are used as a source, it can be calculated the power received for this room by using eq.(3.4) that mention in chapter three.

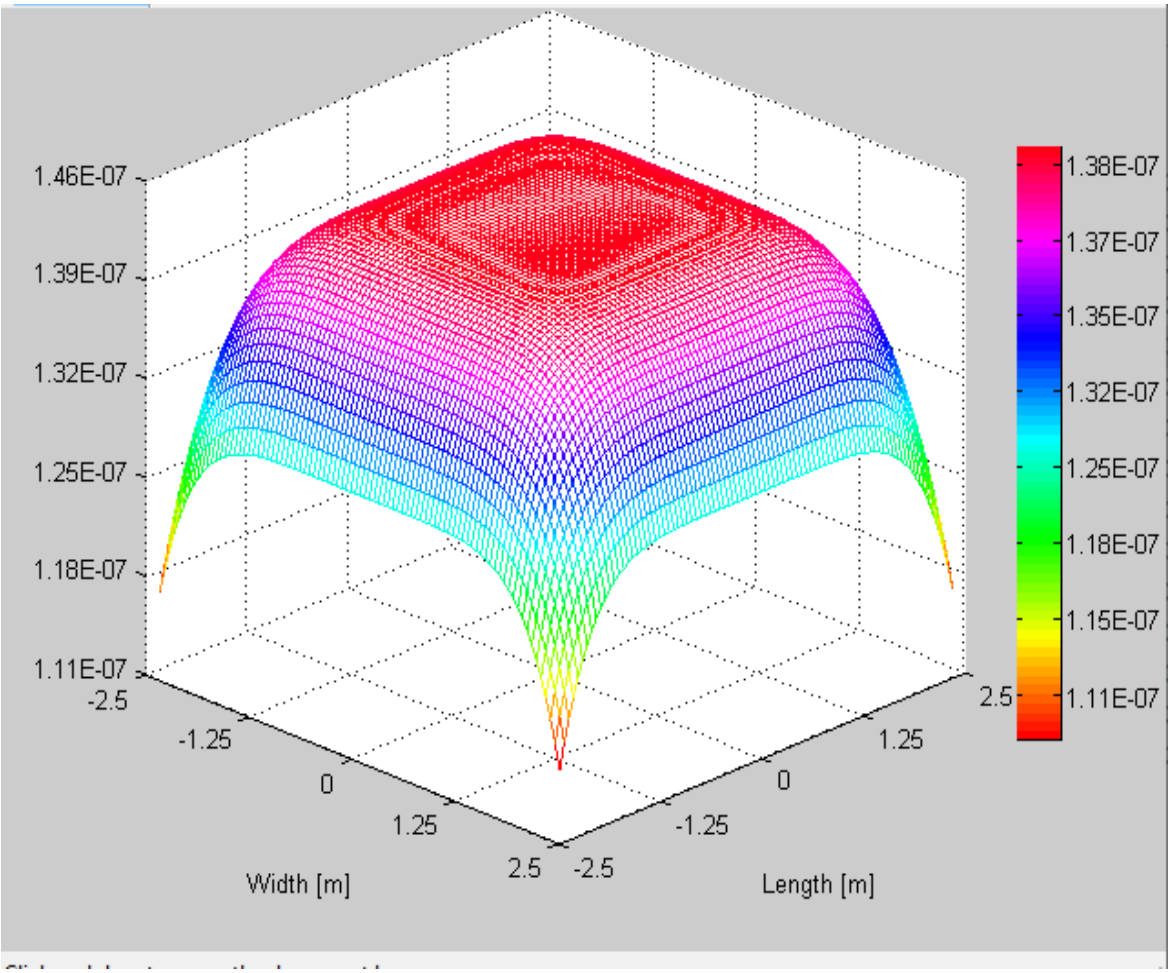

Figure 4.3 A distribution of power receive for 4-LEDs.

However, according to the previous result of received power, it can be calculating the SNR by using eq. (3.10) as mentioned in chapter three.

The SNR signal varies in the range of (44.75 - 44.15) dB for the first quarter in the best point at a testing room, as shown in fig (4.4)

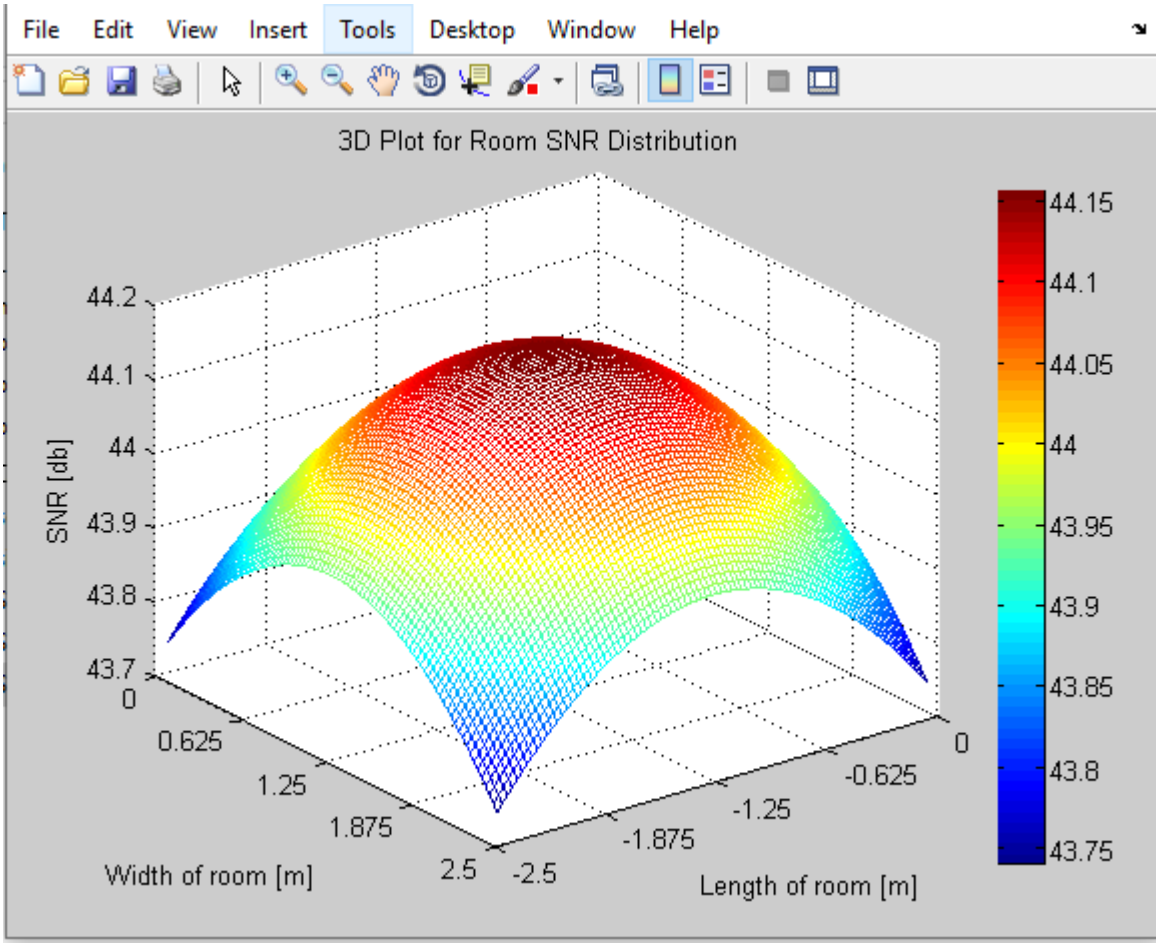

Figure 4.4 3D plot SNR distribution for the first quarter.

The SNR signal varies in the range of (42.40 - 43.45) dB at the testing room, as shown in fig (4.5).

Comparing with the previous result for one researcher the SNR can be reached to 42.5 dB at the better case while the SNR in our work reaches to 43.45 dB at the best point in the room.so, the SNR in our project is higher by (0.95) dB [60] .

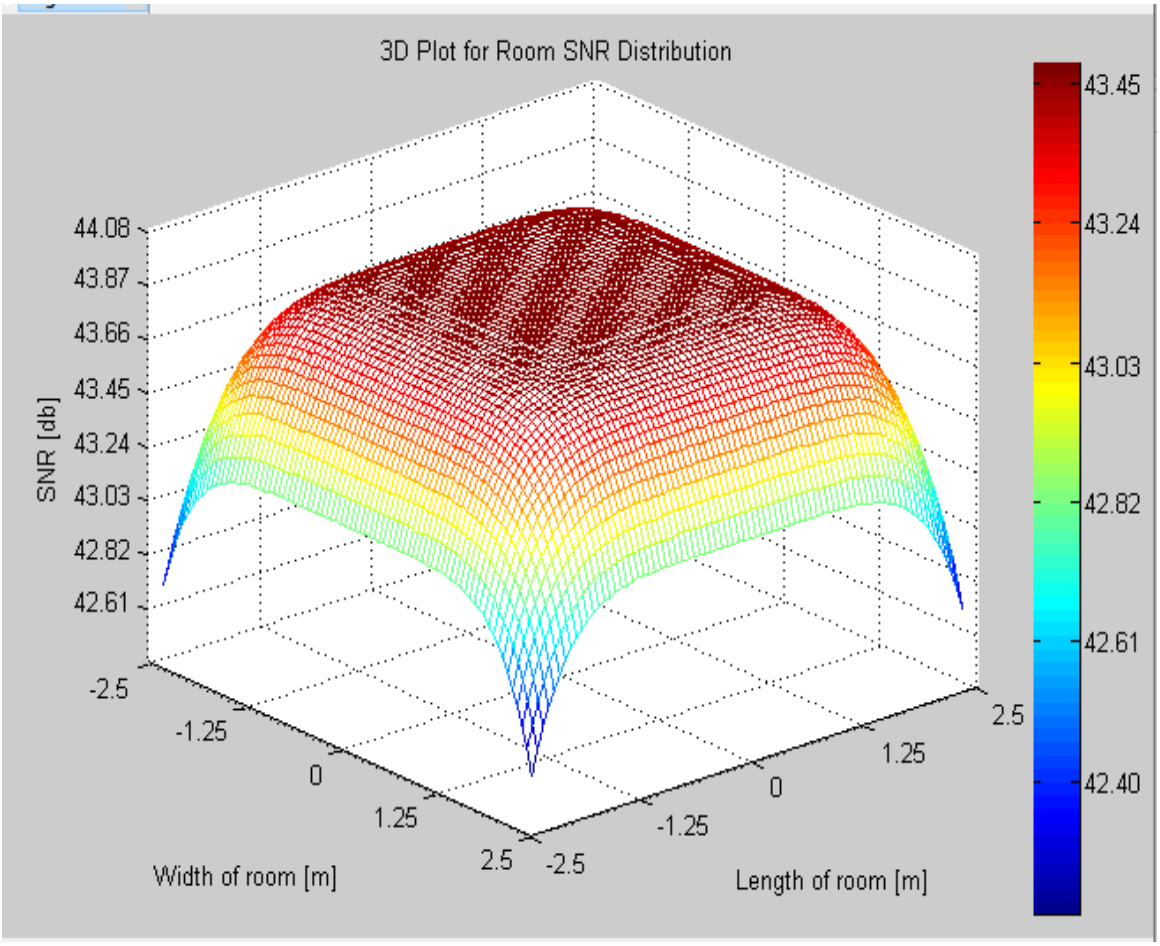

Figure 4.5 3D plot SNR distribution for 4-LEDs.

Table 4.1 shown the arbitral result that has been taken to calculate the SNR for five random positioning.

Table 4.1 shows SNR for five random positioning

Positioning user	X_r-axis[m]	Y_r-axis[m]	Range to source	SNR [dB]
Case 1	1	1	2.52	43.08
Case 2	3	5	2.89	42.89
Case 3	2	2	2.71	43.45

Case 4	1	5	2.80	43.16
Case 5	5	5	3.06	42.40

Compere the result in this work with one research as shown in table 4.2 [58].

Table 4.2 Compared with the results of one research

Cases	SNR (dB) IN 2017	SNR (dB) in this work
Case 1	**40.5**	**43.08**
Case 2	**40.4**	**42.89**
Case 3	**40.2**	**43.45**
Case 4	**27.4**	**43.16**

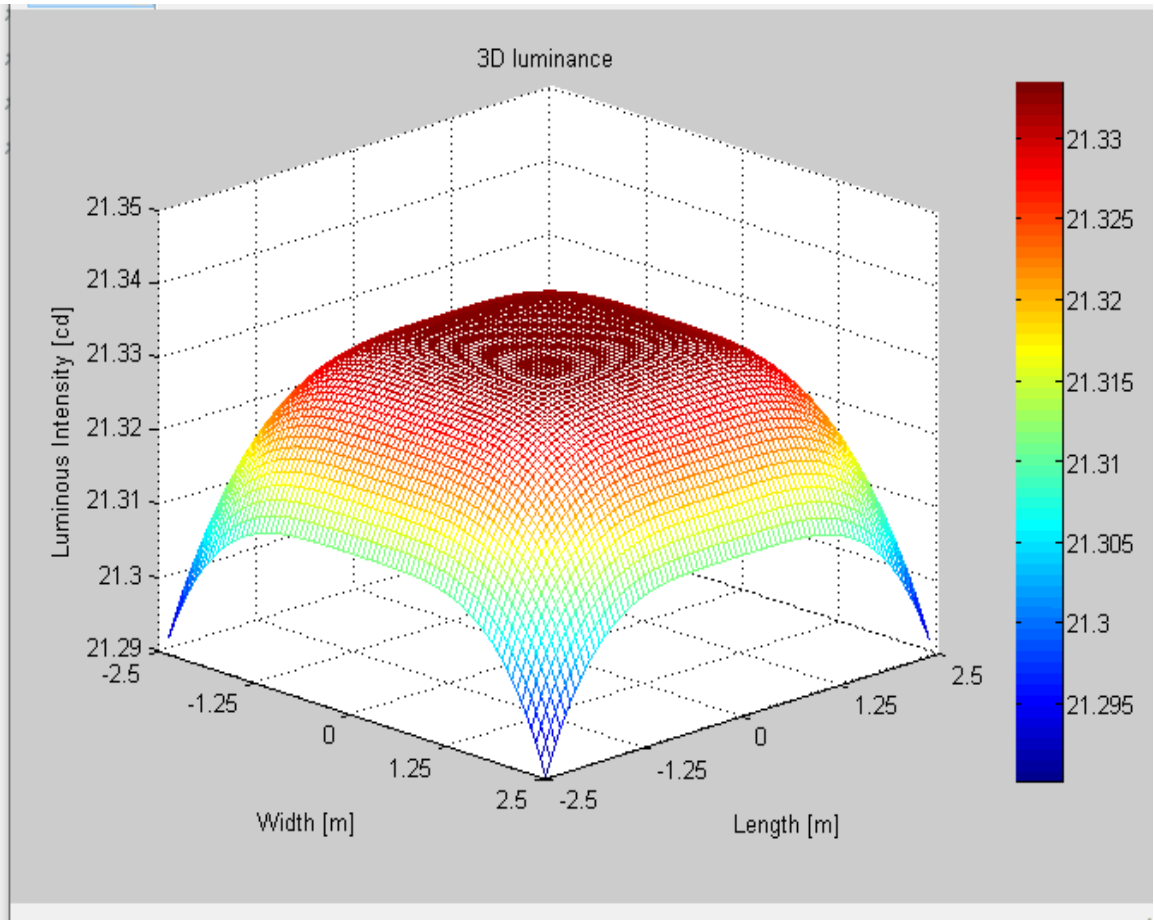

Figure 4.6 The distribution of luminance

The distribution of illuminance for the testing room (5 × 5 × 3) m^3 has shown in fig (4.4). The testing room has considered four LEDs as a source of illuminance, where these value has calculated by using eq.(3.14). So, the range of illuminance that obtained (21.29 – 21.32)cd for the best point in the testing room.

4.3 New Line Neural Network System (NLNNS)

Figure (4.5) illustrate the relationship between SNR Varus BER by using channel coding with different modulation index (M=4). Where are the values of SNR and BER varying with the modulation index as follow :

For M = 4: SNR achieved (30 dB), and BER is higher than 10^{-5}.

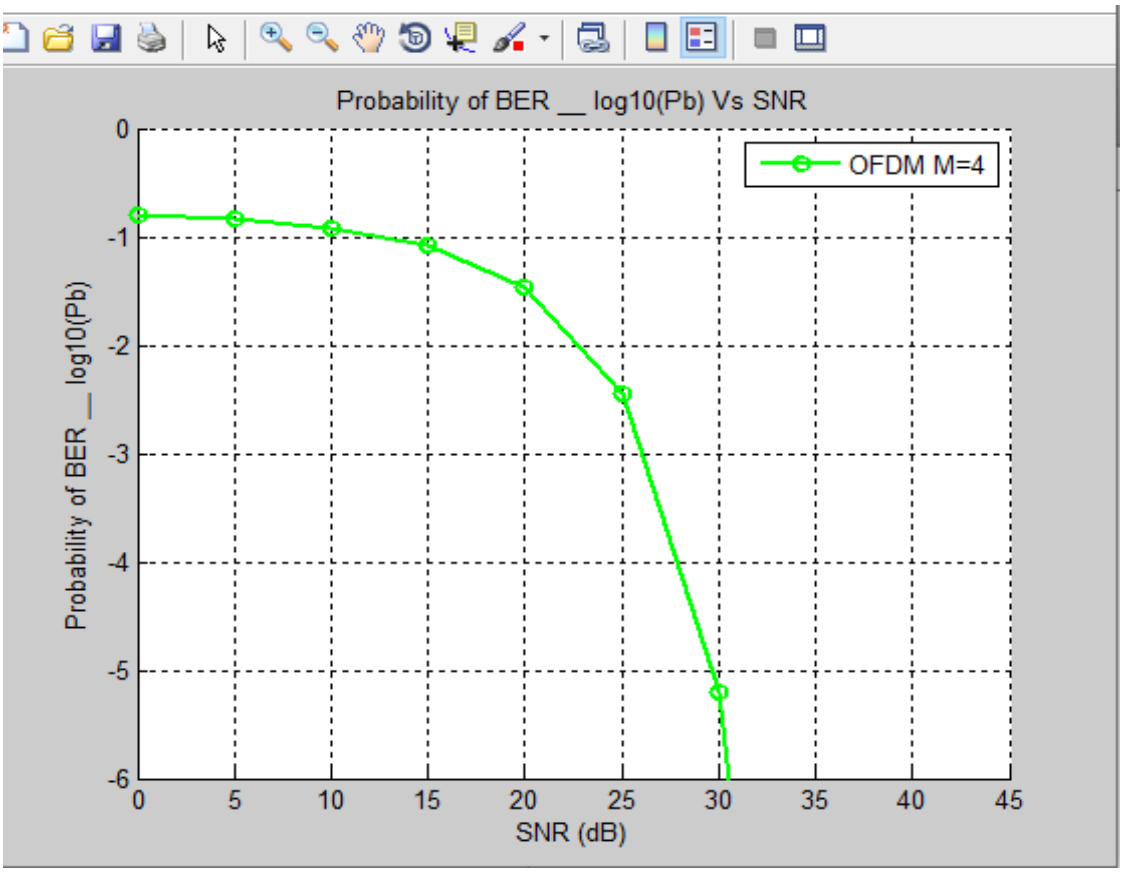

Figure 4.7 The relationship between SNR and BER.

In order to achieve a good verifying between NLNNS algorithm, which are used in this modem system to calculation with other algorithm techniques, we make a compression between NLNNS and OMP algorithm for modulation index M=4 as shown in fig (4.8)

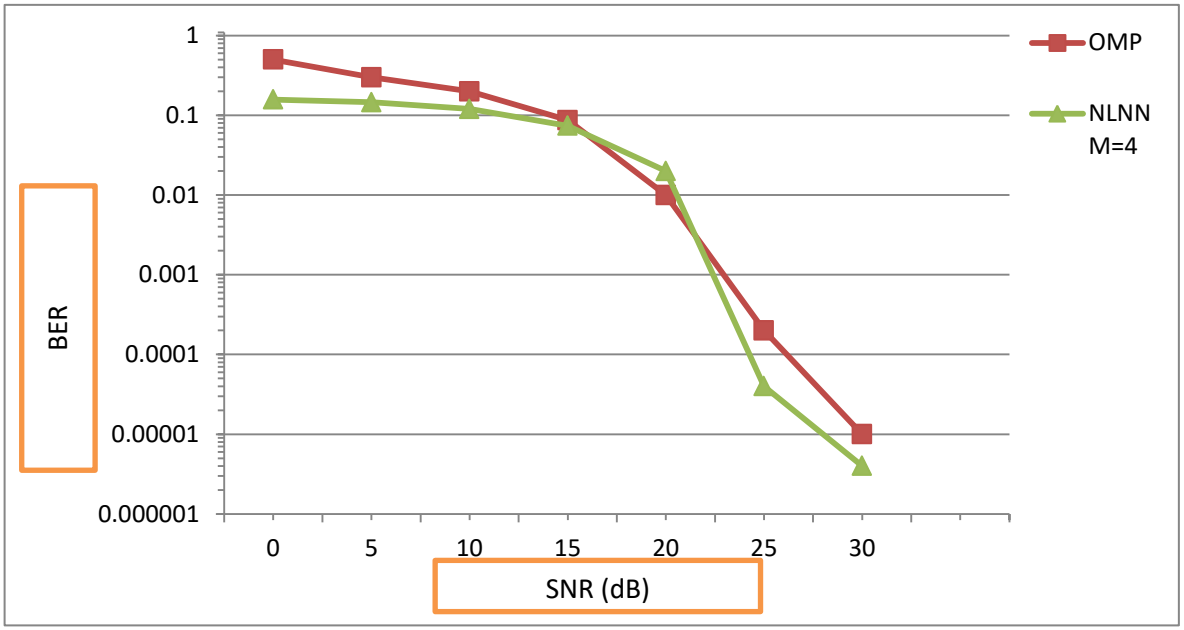

Figure 4.8 Comparing NLNNS and OMP In SNR And BER

It's clear that the OMP algorithm in which SNR and BER values are (30) dB and (10^{-5}) respectively ,while in this algorithm NLNNS the value of SNR is (30) dB and the BER is higher than (10^{-5}) that means this algorithm gives a good result compering with OMP [61].

The SNR obtained in this work is acceptable compared to other work mentioned in [46].

4.4 MIMO-OFDM using NLNNS

Figure (4.9) illustrate the relationship between SNR Varus BER by using MIMO-OFDM in channel coding with different modulation index (M=4,8,16). Where are the values of SNR and BER varying with the modulation index as follow :

For M = 4: SNR achieved (30 dB), and BER is higher than 10^{-5}.

For M = 8: SNR is equal to (40 dB), and BER is higher than 10^{-5}.

For M = 16: SNR is (44.15 dB), and BER is above 10^{-6}.

Where the relationship SNR vs. BER are addressed by eq.(3.32).

according to the result that obtained in our work show the modulation index m=16 is the best performance for SNR and BER

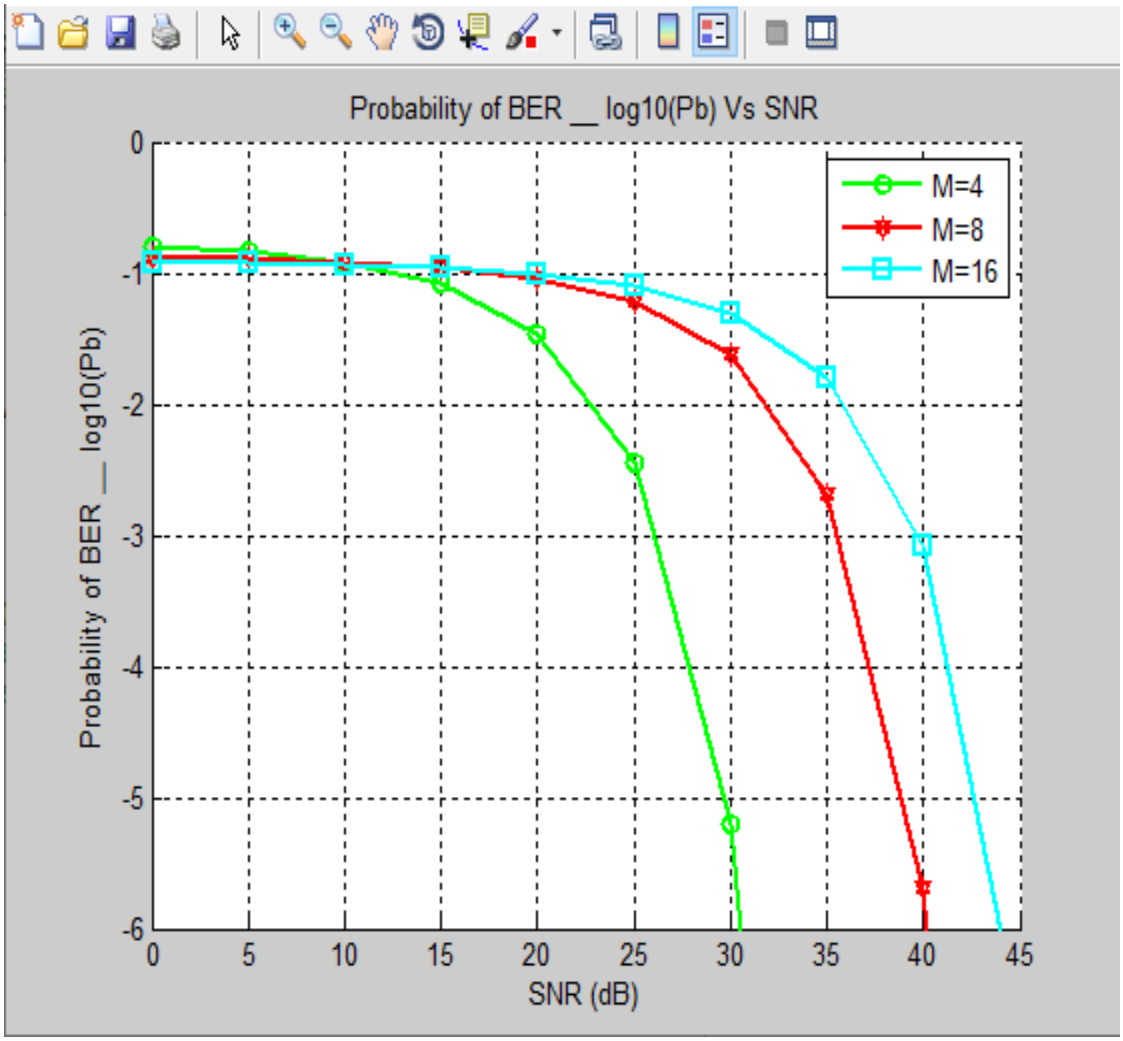

Figure. 4.9 The relationship between SNR and BER for MIMO.

Finally, applying MIMO–OFDM shows many advantages.

First: enhancing the SNR and BER.

Second: eliminate multi-user interference (MUI).

CHAPTER FIVE

CONCLUSIONS AND FUTURE WORKS

5.1. CONCLUSIONS

This work focused on designing and analyzing of the positioning and MIMO-OFDM for the visible light communication under light-emitting diodes (LEDs), where the simulation was carried out in a room with dimensions of 5 m x 5 m x 3 m.

A 3D indoor positioning algorithm system NNCEA which is used the ratio of RSS. Where This proposed system offers high gains of accuracy in a positioning system, furthermore, A 3D positioning results with an average positioning error of less than 20cm in a coverage volume of (5×5x3) m^3 is verified enhancement in SNR and data rate.

On the other hands, the NLNNS algorithm of DFT-S OFDM, which is used to determine the MIMO-OFDM. So, according to the results of BER, we can show the performance of the system within the channel codding has improvement, where the value was more than 10^{-5}. Compared with the results of the OMP method. As well as, the enhancement of SNR has achieved by the value 40 dB and around 44 dB for M=8, 16, respectively. In addition, we elimination of multi-user interference (MUI).

5.2. Future work

In this project, work has been done on visible light communications in positioning and multi-input multi-output. Also, there is a range of topics worth studying in the future.

1) Implement this work in practice.
2) Design and analysis positioning system visible light communications (VLC) based on Frequency Division Multiple Access (FDMA), Code

Division Multiple Access (CDMA) or Hadamard Coded Modulation (HCM).

3) Design and Analysis of Multiple Input and Multiple Output MIMO for Visible Light Communication with the arrangement the LED Positioning and Consider the impact of walls, furniture, shadowing, and sunlight .

Reference

1. Arnon, S., et al., Advanced optical wireless communication systems. 2012: Cambridge university press.
2. Ghassemlooy, Z., W. Popoola, and S. Rajbhandari, Optical wireless communications: system and channel modelling with Matlab®. 2012: CRC press.
3. Medina, C., M. Zambrano, and K. Navarro, Led based visible light communication: Technology, applications and challenges-a survey. International Journal of Advances in Engineering & Technology, 2015. 8(4): p. 482.
4. Bell, A.G., W. Adams, and W. Preece, Discussion on" The photophone and the conversion of radiant energy into sound". Journal of the Society of Telegraph Engineers, 1880. 9(34): p. 375-383.
5. Groth, M., Photophones revisted. Amateur Radio Magazine, 1987: p. 12-17.
6. Jackson, D.K., T.K. Buffaloe, and S.B. Leeb, Fiat lux: A fluorescent lamp digital transceiver. IEEE Transactions on industry applications, 1998. 34(3): p. 625-630.
7. Bouchet, O., et al. Hybrid wireless optics (HWO): Building the next-generation home network. in 2008 6th International Symposium on Communication Systems, Networks and Digital Signal Processing. 2008. IEEE.
8. Kulhavy, K., FPGA-Based RONJA Twister,. 2012, RONJA.
9. Tanaka, Y., et al., Indoor visible light data transmission system utilizing white LED lights. IEICE transactions on communications, 2003. 86(8): p. 2440-2454.
10. Vučić, J., et al., 513 Mbit/s visible light communications link based on DMT-modulation of a white LED. Journal of lightwave technology, 2010. 28(24): p. 3512-3518.
11. Burton, A., et al. A study of LED lumination uniformity with mobility for visible light communications. in 2012 international workshop on optical wireless communications (IWOW). 2012. IEEE.

12. Wang, Z., et al., Performance of a novel LED lamp arrangement to reduce SNR fluctuation for multi-user visible light communication systems. Optics express, 2012. 20(4): p. 4564-4573.

13. Chun, H., et al., A study of illumination and communication using organic light emitting diodes. Journal of Lightwave Technology, 2013. 31(22): p. 3511-3517.

14. Azizan, L.A.-H., M.S. Ab-Rahman, and K. Jumiran. Analytical approach on SNR performance of visible light communication for modern lighting layout. in 2012 International Conference on Innovation Management and Technology Research. 2012. IEEE.

15. Chow, C.-W., et al., A practical in-home illumination consideration to reduce data rate fluctuation in visible light communication. IEEE Wireless Communications, 2015. 22(2): p. 17-23.

16. Ding, J., Z. Huang, and Y. Ji, Evolutionary algorithm based uniform received power and illumination rendering for indoor visible light communication. JOSA A, 2012. 29(6): p. 971-979.

17. Y. He, L. Ding, Y. Gong, and Y. Wang, \Real-time audio & video transmission system based on visible light communication," Optics and Photonics Journal, vol. 3, no. 02, p. 153, 2013.

18. T. Yamazato, I. Takai, H. Okada, T. Fujii, T. Yendo, S. Arai, M. Andoh, T. Harada, K. Yasutomi, K. Kagawa et al., \Image-sensor-based visible light communication for automotive applications," I EEE Communications Magazine, vol. 52, no. 7, pp. 88{97, 2014.

19. J. Luo, L. Fan, and H. Li, "Indoor Positioning Systems Based on Visible Light Communication: State of the Art," IEEE Commun. Surveys Tuts., vol. 19, no. 4, pp. 2871-2893, 2017.

20. B. Lin, X. Tang, Z. Ghassemlooy, C. Lin, and Y. Li, “Experimental demonstration of an indoor VLC positioning system based on OFDMA,” IEEE Photon. J., vol. 9, pp. 19, 2017.

21. H. B. Demuth, M. H. Beale, O. De Jess, and M. T. Hagan, Neural network design. Martin Hagan, 2014.

22. Armstrong, J., OFDM for optical communications. Journal of lightwave technology, 2009. 27(3): p. 189-204.
23. Wu, Z.-Y., et al., Modulation index dependence of intensity modulation bandwidth in visible light communications. Optics letters, 2018. 43(19): p. 4570-4573.
24. Gao, Y.-L., et al., A 1.34-Gb/s Real-Time Li-Fi Transceiver With DFT-Spread-Based PAPR Mitigation. IEEE Photonics Technology Letters, 2018. 30(16): p. 1447-1450.
25. Kuo, P.-H., H. Kung, and P.-A. Ting. Compressive sensing based channel feedback protocols for spatially-correlated massive antenna arrays. in IEEE Wireless Communications and Networking Conference (WCNC). 2012. IEEE.
26. Wang, Y., et al., Enhanced performance of visible light communication employing 512-QAM N-SC-FDE and DD-LMS. Optics express, 2014. 22(13): p. 15328-15334.
27. Perez-Jimenez, R., et al. Visible light communication systems for passenger in-flight data networking. in 2011 IEEE International Conference on Consumer Electronics (ICCE). 2011. IEEE.
28. Rajbhandari, S., Z. Ghassemlooy, and M. Angelova, Wavelet—Artificial neural network receiver for indoor optical wireless communications. Journal of lightwave technology, 2011. 29(17): p. 2651-2659.
29. Lee, H., I. Lee, and S.H. Lee, Deep learning based transceiver design for multi-colored VLC systems. Optics express, 2018. 26(5): p. 6222-6238.
30. Pope, G., Compressive sensing: A summary of reconstruction algorithms. 2009, ETH, Swiss Federal Institute of Technology Zurich, Department of Computer ….
31. Tsonev, D. and H. Haas. Avoiding spectral efficiency loss in unipolar OFDM for optical wireless communication. in IEEE international conference on communications (ICC). 2014. IEEE.
32. Wang, Q., Z. Wang, and L. Dai, Multiuser MIMO-OFDM for visible light communications. IEEE Photonics Journal, 2015. 7(6): p. 1-11.
33. Basar, E., Index modulation techniques for 5G wireless networks. IEEE Communications Magazine, 2016. 54(7): p. 168-175.
34. Mesleh, R., H. Elgala, and H. Haas, Optical spatial modulation. Journal of Optical Communications and Networking, 2011. 3(3): p. 234-244.

35. Grubor, J., et al., High-Speed Wireless Indoor Communication via Visible Light; Itg-Fachbericht Breitbandversorgung in Deutschland—Vielfalt Fur Alle. 2007, VDE Verlag: Berlin, Germany.
36. Lee, K., H. Park, and J.R. Barry, Indoor channel characteristics for visible light communications. IEEE communications letters, 2011. 15(2): p. 217-219.
37. Zhang, W. and M. Kavehrad. Comparison of VLC-based indoor positioning techniques. in Broadband Access Communication Technologies VII. 2013. International Society for Optics and Photonics.
38. Ghassemlooy, Z., et al., Indoor nondirected optical wireless communications—Optimization of the Lambertian order. J. Elect. Comput. Eng. Innov, 2013. 1(1): p. 1-9.
39. Tan, J., et al., Simulation of MIMO channel characteristics for indoor visible light communication with LEDs. Optik, 2014. 125(1): p. 44-49.
40. Zhang, W., M.S. Chowdhury, and M. Kavehrad, Asynchronous indoor positioning system based on visible light communications. Optical Engineering, 2014. 53(4): p. 045105.
41. Pathak, P.H., et al., Visible light communication, networking, and sensing: A survey, potential and challenges. IEEE communications surveys & tutorials, 2015. 17(4): p. 2047-2077.
42. Wu, L., et al., Adaptive modulation schemes for visible light communications. Journal of Lightwave Technology, 2014. 33(1): p. 117-125.
43. Zhou, Y., et al. MIMO VLC positioning system based on LEDs utilizing diversity reception technology. in 2015 International Conference on Wireless Communications & Signal Processing (WCSP). 2015. IEEE.
44. Son, T.T., et al. Adaptive correction model for indoor MIMO VLC using positioning technique with node knowledge. in 2015 International Conference on Communications, Management and Telecommunications (ComManTel). 2015. IEEE.
45. He, C., T.Q. Wang, and J. Armstrong, Performance of optical receivers using photodetectors with different fields of view in a MIMO ACO-OFDM system. journal of Lightwave Technology, 2015. 33(23): p. 4957-4967.

46. Yesilkaya, A., et al., Optical MIMO-OFDM with generalized LED index modulation. IEEE Transactions on Communications, 2017. 65(8): p. 3429-3441.
47. Fuada, S., A.P. Putra, and T. Adiono, Analysis of received power characteristics of commercial photodiodes in indoor LoS channel visible light communication. Int. J. of Advanced Computer Science and Applications, 2017. 8(7): p. 164-172.
48. Wang, Y., X. Wu, and H. Haas. Resource allocation in LiFi OFDMA systems. in GLOBECOM 2017-2017 IEEE Global Communications Conference. 2017. IEEE.
49. Al-Nassrawi, M., et al. Indoor positioning using single transmitter for visible light communications system. in 2017 First South American Colloquium on Visible Light Communications (SACVLC). 2017. IEEE.
50. Gligorić, K., et al., Visible light communications-based indoor positioning via compressed sensing. IEEE Communications Letters, 2018. 22(7): p. 1410-1413.
51. Lin, C., et al. An Indoor Visible Light Positioning System Using Artificial Neural Network. in 2018 Asia Communications and Photonics Conference (ACP). 2018. IEEE.
52. Zhang, S., et al. 3D Indoor visible light positioning system using RSS ratio with neural network. in 2018 23rd Opto-Electronics and Communications Conference (OECC). 2018. IEEE.
53. Lorrière, N., et al. An OFDM testbed for LiFi performance characterization of photovoltaic modules. in 2018 Global LIFI Congress (GLC). 2018. IEEE.
54. Akande, K.O., et al. Performance Comparison of MIMO CAP Receivers in Visible Light Communication. in 2018 11th International Symposium on Communication Systems, Networks & Digital Signal Processing (CSNDSP). 2018. IEEE.
55. Chen, C., et al., On the performance of MIMO-NOMA-based visible light communication systems. IEEE Photonics Technology Letters, 2017. 30(4): p. 307-310.

56. Bian, R., I. Tavakkolnia, and H. Haas, 15.73 Gb/s Visible Light Communication with off-the-shelf LEDs. Journal of Lightwave Technology, 2019. 37(10): p. 2418-2424.
57. Soltani, M.D., et al., Impact of device orientation on error performance of LiFi systems. IEEE Access, 2019. 7: p. 41690-41701.
58. Prasithsangaree, P., P. Krishnamurthy, and P. Chrysanthis. On indoor position location with wireless LANs. in The 13th IEEE international symposium on personal, indoor and mobile radio communications. 2002. IEEE.
59. Elganimi, T.Y., Performance comparison between OOK, PPM and pam modulation schemes for free space optical (FSO) communication systems: analytical study. International Journal of Computer Applications, 2013. 79(11).
60. Huanhuan, Z., Design And Analysis Of Visible Light Communication And Positioning Systems,in 2017.
61. Gao, Y.-l., Z.-Y. Wu, and J. Wang, Convolution neural network-based time-domain equalizer for DFT-Spread OFDM VLC system. Optics Communications, 2019. 435: p. 35-40.

Appendix A1

NNCEA Algorithm for Positioning in VLC

```
% xr = xaxisformobile;
% yr = yaxisformobile;
% zr = zaxisformobile;
% xs = xaxisforsource;
% ys = yaxisforsource;
% zs = zaxisforsource;
% L=lengthofroominmeter;
% W=widthofroominmeter;
% xs=0,ys=0,zs=0 at source;
clear all
close all
clc
zs=input('input zs= ');
 L= input('input L= ');
 W= input('input w= ');
zr=input('input zr= ');

% r=L*2*W*2;

% Learning for Position Matrix

k=1;
z=(zs-zr);
 xs1=W/4;  ys1=-L/4;  xs2=(3*W)/4; ys2=-L/4; xs3=W/4; ys3=(-3*L)/4;
xs4=(3*W)/4;  ys4=(-3*L)/4;

d(k,1)=1;d(k,2)=2;d(k,3)=3;d(k,4)=4;
k=k+1;
for s=1:1:4;

            if (s==1)
                    ww=0;
                    ll=0;
                    ws=W/2;
                    ls=-L/2;
                    xs=xs1;
                    ys=ys1;
            elseif (s==2)
                    ww=W/2;
                    ll=0;
                    ws=W;
                    ls=-L/2;
                     xs=xs2;
                     ys=ys2;
            elseif (s==3)
                    ww=0;
                    ll=-L/2;
                    ws=W/2;
```

```
                    ls=-L;
                    xs=xs3;
                    ys=ys3;

            else
                   ww=W/2;
                   ll=-L/2;
                   ws=W;
                   ls=-L;
                   xs=xs4;
                   ys=ys4;
            end

for i=ww:0.5:ws;
for j=ll:-0.5:ls;

        x11=i-xs;
        y11=(j-ys);
    rr1=sqrt(x11^2+y11^2+z^2);
    d(k,1)=rr1;
    d(k+1,1)=x11;
    d(k+2,1)=y11;
    k=k+3;
end

end
end

% Positioning

xr=input('input xr= ');
yr=-input('input yr= ');
qr=0;

           if (xr<=W/2 && yr>=-L/2)
                   ww=0;
                   ll=0;
                   ws=W/2;
                   ls=-L/2;
                   xs=xs1;
                   ys=ys1;
                   sr='S1';
                   qr=1;
            elseif (xr>W/2 && yr>-L/2)
                   ww=W/2;
                   ll=0;
                   ws=W;
                   ls=-L/2;
                    xs=xs2;
                   ys=ys2;
                    sr='S2';
                    qr=2;
            elseif (xr<=W/4 && yr>=-L)
                   ww=0;
                   ll=-L/2;
```

```
                    ws=W/2;
                    ls=-L;
                    xs=xs3;
                    ys=ys3;
                    sr='S3';
                    qr=3;
            else
                    ww=W/2;
                   ll=-L/2;
                   ws=W;
                   ls=-L;
                   xs=xs4;
                    ys=ys4;
                    sr='S4';
                    qr=4;
           end


% Calculate the source number
i=580*10^(-9);
gs=1;
gr= 1;
ps= 0.02;
% Photodiode responsivity (A/W )%
R = 0.5;

% Si
x11=xr-xs;
y11=yr-ys;
rr1=sqrt(x11^2+y11^2+z^2);
pe=(ps*gs*gr*i*(R/(rr1*4*pi))^2);


xx1=xr-xs1;
yy1=yr-ys1;
rr1=sqrt(xx1^2+yy1^2+z^2);
pe1=(ps*gs*gr*i*(R/(rr1*4*pi))^2);
phi=85;
m = -log(2)/log(cos(phi)); % Order of Lambertian emission %
ARX = (0.5*10^-3);
Ro1 = ps*((m+1)*ARX/(2*pi*rr1^2))*cos(phi)^m+1; % Lambertian radiant
intensity %


xx2=xr-xs2;
yy2=yr-ys2;
rr2=sqrt(xx2^2+yy2^2+z^2);
pe2=(ps*gs*gr*i*(R/(rr2*4*pi))^2);
phi=85;
m = -log(2)/log(cos(phi)); % Order of Lambertian emission %
ARX = (0.5*10^-3);
Ro2 = ps*((m+1)*ARX/(2*pi*rr2^2))*cos(phi)^m+1; % Lambertian radiant
intensity %
```

```
xx3=xr-xs3;
yy3=yr-ys3;
rr3=sqrt(xx3^2+yy3^2+z^2);
pe3=(ps*gs*gr*i*(R/(rr3*4*pi))^2);
phi=85;
m = -log(2)/log(cos(phi)); % Order of Lambertian emission %
ARX = (0.5*10^-3);
Ro3 = ps*((m+1)*ARX/(2*pi*rr3^2))*cos(phi)^m+1; % Lambertian radiant
intensity %


xx4=xr-xs4;
yy4=yr-ys4;
rr4=sqrt(xx4^2+yy4^2+z^2);
pe4=(ps*gs*gr*i*(R/(rr4*4*pi))^2);
phi=85;
m = -log(2)/log(cos(phi)); % Order of Lambertian emission %
ARX = (0.5*10^-3);
Ro4 = ps*((m+1)*ARX/(2*pi*rr4^2))*cos(phi)^m+1; % Lambertian radiant
intensity %

% %
 if (xx1==x11 && yy1==y11)
    ratio1= (((Ro3+Ro4)/2)/Ro1);
elseif (xx2==x11 && yy2==y11)
    ratio2= (((Ro2+Ro4)/2)/Ro2);
elseif (xx3==x11 && yy3==y11)
   ratio3= (((Ro1+Ro4)/2)/Ro3);
else
   ratio4= (((Ro2+Ro3)/2)/Ro4);
end
%
%  ratio1= ((Ro1/(Ro3+Ro4)/2));
%  ratio2= ((Ro2/(Ro2+Ro4)/2));
%  ratio3= ((Ro3/(Ro1+Ro4)/2));
%  ratio4= ((Ro4/(Ro2+Ro3)/2));
%
% % % k=2;
% % % % for i=0:0.5:W;
% % % % for j=0:0.5:L;
% % %
% % %
% % %             if (x11<=W/4 && y11>=-L/4)
% % %                     sr='S1';
% % %                     pe=(ps*gs*gr*i*(R/(rr1*4*pi))^2);
% % %
% % %             elseif (x11<=(3*W)/4 && y11>=-L/4)
% % %                     sr=2;
% % %                     pe= (ps*gs*gr*i*(R/(rr2*4*pi))^2);
% % %
% % %             elseif (x11<=W/4 && y11>=(-3*L)/4)
% % %                     sr=3;
% % %                     pe= (ps*gs*gr*i*(R/(rr3*4*pi))^2);
% % %
% % %             else
% % %                     sr=4;
```

```
% % %                     pe= (ps*gs*gr*i*(R/(rr4*4*pi))^2);
% % %
% % %             end
% end
% end


% Noise-bandwidth factor %
I2 = 0.562;
% Data rate (Bit per second)
Rb = 115200;
% Ambient light power (Ampere) %
Iamb = 7E-8;
% Photodiode responsivity (A/W )%
R = 0.5;
% Electron charge (C)
q = 1.60E-19;
% Amplifier bandwidth (Hz)%
Ba = 4.5E6;
% Amplifier noise density (Ampere/Hz^0.5)%
Iamf = 5e-12 ;
 Prx_total= 1.0636e-09;
 Bn = I2 * Rb; % Noise-bandwidth (Sec^-1)%
Pamb = Iamb / R; % Ambient light power (W) %
% Shot-noise variance ( Ampere^2 )%
omega_shot = 2 * q * R * (Prx_total + Pamb) * Bn;
% Amplifier noise variance ( Ampere^2 )%
omega_amplifier = Iamf^2 * Ba;
% Total noise variance ( Ampere^2 )%
omega_total = omega_amplifier + omega_shot;

% pe= (ps*gs*gr*i*(R/(rr*4*pi))^2);

SNR1 =  pe1/ omega_total;
SNR1dB = (10 * log10(SNR1)); % SNR in dB %


SNR2 =  pe2 / omega_total;
SNR2dB = (10 * log10(SNR2)); % SNR in dB %

SNR3 =  pe3 / omega_total;
SNR3dB = (10 * log10(SNR3)); % SNR in dB %

SNR4 =  pe4 / omega_total;
SNR4dB = (10 * log10(SNR4)); % SNR in dB %
```

Appendix A2

LMS (Least means square)

```
% function [e,w]=lms(mu,M,u,d);

% Call:

 %     [e,w]=lms(mu,M,u,d);

 % Input arguments:

% mu = step size, dim 1x1

 % M = filter length, dim 1x1

% u = input signal, dim Nx1

 % d = desired signal, dim Nx1

 % Output arguments:

 % e = estimation error, dim Nx1 %

 w = final filter coefficients, dim Mx1

%inital values: 0

 w=zeros(M,1);

%number of samples of the input signal

N=length(u);

%Make sure that u and d are column vectors

 u=u(:);

 d=d(:);

%LMS

 for n=M:N uvec=u(n:-1:n-M+1);

e(n)=d(n)-w'*uvec; w=w+mu*uvec*conj(e(n));

 end

e=e(:);
```

```
% filter coefficients
h=0.5.^[0:4];
 % input signal
u=randn(1000,1);
 % filtered input signal == desired signal
 d=conv(h,u);
 % LMS
[e,w]=lms(0.1,5,u,d);
```

Appendix B

NLNNS Algorithm for MIMO_OFDM in VLC

```
clc;
close all;
EbN0dB=0:5:45;
EbN0lin=10.^(EbN0dB/10);
colors={'k-*','g-o','r-h','c-s','m-s','y-*','k-p','b:s','m:d','g:p'};
index=1;

% % %BPSK
% %
% BPSK = 0.5*erfc(sqrt(EbN0lin));
% plotHandle=plot(EbN0dB,log10(BPSK),char(colors(index)));
% set(plotHandle,'LineWidth',1.5);
hold on;

index=index+1;

%% Transmitter


% data generation
Tx_data=randi([0 1024],L,Ncp);
%%%%%%%%%%%%%%%%%%%% QAM modulation %%%%%%%%%%%%%%%%%%%%
mod_data=qammod(Tx_data,2048);
% Serial to Parallel
s2p=mod_data.';
% IFFT
am=ifft(s2p);
% Parallel to series
p2s=am.';
% Cyclic Prefixing
CP_part=p2s(:,end-Ncp+1:end); %Cyclic Prefix part to be appended.
cp=[CP_part p2s];

m=10.9;
M=2.^m;

for i=M,
    k=log2(i);
    berErr = 2/k*(1-1/sqrt(i))*erfc(sqrt(3*EbN0lin*k/(2*(i-1))));
    plotHandle=plot(EbN0dB,log10(berErr),char(colors(index)));
    set(plotHandle,'LineWidth',1.5);
    index=index+1;
end



for i=M,
    k=log2(i);
```

```
        berErr = 2/k*(1-1/sqrt(i))*erfc(sqrt(3*EbN0lin*k/(2*(i-1))));
        plotHandle=plot(EbN0dB,log10(berErr),char(colors(index)));
        set(plotHandle,'LineWidth',1.5);
Reciever

% Adding Noise using AWGN
r=zeros(size(SNRstart:SNRincrement:SNRend));
for snr=SNRstart:SNRincrement:SNRend
    c=c+1;
    noisy=awgn(cp,snr,'measured');
% Remove cyclic prefix part
    cpr=noisy(:,Ncp+1:Ncp+Ncp); %remove the Cyclic prefix
% series to parallel
    parallel=cpr.';
% FFT
    amdemod=fft(parallel);
% Parallel to serial
    rserial=amdemod.';
%%%%%%%%%%%%%%%%%%%% QAM demodulation %%%%%%%%%%%%%%%%%%%%
    Umap=qamdemod(rserial,2048);
% Calculating the Bit Error Rate
    [n, r(c)]=biterr(Tx_data,Umap);

end
snr=SNRstart:SNRincrement:SNRend;

      index=index+1;
    end

    for i=M,
        k=log2(i);
        berErr = 2/k*(1-1/sqrt(i))*erfc(sqrt(3*EbN0lin*k/(2*(i-1))));
        plotHandle=plot(EbN0dB,log10(berErr),char(colors(index)));
        set(plotHandle,'LineWidth',1.5);
        index=index+1;
    end


    legend('M=4','M=8','M=16');
    axis([0 45 -6 0]);
    set(gca,'XTick',0:5:45);
    ylabel('Probability of BER __ log10(Pb)');
    xlabel('SNR (dB)');
    title('Probability of BER __ log10(Pb) Vs SNR');
    grid on;
```